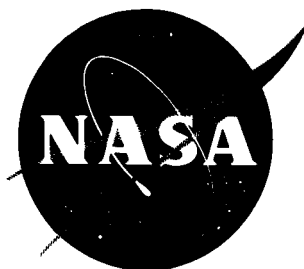


7N-26

195552

648.



# TECHNICAL NOTE

## D-109

EFFECTS OF CREEP STRESS ON PARTICULATE  
ALUMINUM-COPPER ALLOYS

By E. E. Underwood and G. K. Manning

Battelle Memorial Institute

NATIONAL AERONAUTICS AND SPACE ADMINISTRATION  
WASHINGTON

September 1959

(NASA-TN-D-109) EFFECTS OF CREEP STRESS ON  
PARTICULATE ALUMINUM-COPPER ALLOYS  
(Battelle Memorial Inst.) 64 p

N89-70610

Unclas  
00/26 0195552

## NATIONAL AERONAUTICS AND SPACE ADMINISTRATION

## TECHNICAL NOTE D-109

## EFFECTS OF CREEP STRESS ON PARTICULATE

## ALUMINUM-COPPER ALLOYS

By E. E. Underwood and G. K. Manning

## SUMMARY

Particle dissolution, grain growth, and precipitation were studied under creep conditions in overaged alloys of aluminum with 1, 2, 3, and 4 percent copper. Particle dissolution, with or without stress, is described by the same kinetic equation that applies to tempering and other phase transformations. The activation energy for dissolution in 3-percent-copper alloys decreases from 70 kcal/mol without stress to 40 kcal/mol for a stress of 200 psi. Relative activation energies for particle dissolution and grain growth coincide closely, suggesting that both are governed by the same process. At a constant stress, the volume of precipitate depends only on the strain, independent of the times or temperatures involved. Grain growth, with and without stress, obeys the equation offered by Beck. A retardation of growth rates in alloys with 2 percent copper is believed to be related to a retardation in rate of age hardening and an increased creep resistance found previously in the same alloys. A good correspondence between measured and calculated grain sizes is obtained with Zener's expression relating particle size to grain size.

## INTRODUCTION

Most theories of particle hardening in alloys assume the presence of hard, spherical particles of uniform size, randomly distributed throughout a softer matrix. A more realistic picture would take into account particles with other than spherical shape, a size distribution of particles, preferred locations where particle density is high, and particles that deform to some extent under load. The complexities attendant to such a detailed consideration are truly prohibitive, but by the proper choice of model, which would take into account the important features of the process, significant simplification may be attained.

Before these more realistic theories can be developed, however, it is necessary to have some background of experimental fact, especially under high-temperature conditions. The problem encountered with

high-temperature deformation is that additional variables are introduced which must also be considered. Paramount in this regard is the enhanced rate of diffusion, to which may be traced almost all of the instabilities of a stressed metal or alloy. Recovery and recrystallization, grain growth, particle dissolution and stress-induced precipitation, polygonization and formation of subgrains, equilibrium or nonequilibrium solute segregation, phase transformations, void formation - these and other processes may be operative in a stressed metal at high temperatures.

The research described herein represents an attempt to isolate and study quantitatively, whenever possible, some of these more important instability processes. Grain growth and particle dissolution, both with and without an applied stress, have been given primary emphasis in this phase of the study. Some attention has been paid to the effect of stress on inducing additional precipitation, frequently in amounts beyond that predicted by the phase diagram. The ultimate goal of this investigation is to relate the effects of the individual processes to the case where all are operating simultaneously. In this way, it is hoped to better understand those factors which are of primary importance in defining the strength of particulate alloys at elevated temperatures.

W  
1  
1  
9

This investigation was conducted at the Battelle Memorial Institute under the sponsorship and with the financial assistance of the National Advisory Committee for Aeronautics. The assistance of Mr. R. D. Smith was of great help throughout the entire investigation. Thanks are also due Mr. John Schroeder for the X-ray results, and Mr. L. L. Marsh for discussion of the data.

## BACKGROUND

Many reviews and articles on the strength of particulate alloys are available in the literature (ref. 1). The theories and experimental work pertinent to this investigation have been reviewed in reference 2 and the discussion will not be repeated here; however, the main findings from the previous investigations leading up to the work reported herein will be described briefly.

In 1955, the interrelation of creep and age hardening was investigated in aluminum-copper alloys (ref. 3). It was found that the amount of precipitation induced by aging during creep was about 2 to 3 times greater than that occurring in unstressed alloys. Abundant evidence supporting the existence of this small-particle effect was found in the literature and from such diverse sources as X-ray measurements, photomicrographs, dilatometer measurements, and other quantitative metallographic studies. To explain this result, it was suggested that the small initial precipitate had less than the expected solute concentration.

The effects of creep stress on the aging rate were also investigated. The time to maximum hardness was decreased by increased stress, but the maximum hardness occurred at the same strain, regardless of the magnitude of the stress. Furthermore, the level of the hardness curves varied directly with the stress, as did the tensile flow stress of crept alloys. The emergence of the strain, rather than the aging time, as the primary variable was demonstrated clearly. Other results to be described in this report also substantiate the latter finding.

W  
1  
1  
9 Some interesting and unusual aspects of high-temperature behavior were revealed by so-called "contour" plots. Lines of equal value of some property are superimposed on the appropriate portion of the phase diagram, revealing their variation with composition and temperature. Contours of equal time to maximum hardness were constructed from aging data over a composition range of 1 to 4 percent copper and a temperature range that included the two-phase region. Two noteworthy facts emerged: (1) The curve of maximum rate of age hardening runs parallel to and about 70° C below the solvus boundary, and (2) a region of retarded rate of age hardening occurs near the 2-percent-copper compositions at about 300° C. This region of retardation is of especial interest because it was found that the creep resistance increased appreciably in 2-percent-copper alloys at 300° C. In another system where diffusion data were available, the region of retardation was found to coincide with a greatly reduced rate of diffusion. Thus, the temperature and composition range which is associated with a relative increase in creep resistance can be found from simple aging curves.

The relative creep resistance of single- and two-phase alloys were compared over a wide range of temperatures and stresses. The curve for single-phase alloys was extrapolated into the two-phase region by means of a temperature-minimum creep rate parameter. It was found that at the intermediate stresses, the two-phase alloys were stronger than the single-phase alloys of the same overall composition; however, at the extremes of temperature and stress, the single-phase alloys tended to become stronger. This prediction has received experimental verification from reports in the literature. The conclusion was reached that matrix strengthening contributes appreciably to the overall strength of the alloy.

The two-phase alloys described above were initially single-phase, then aged during creep. The research programmed for 1956 (ref. 2) dealt with aluminum-copper alloys in which the precipitate particles were present before the creep test. By special heat treatments large spherical particles or large platelike particles were formed, and such characteristics as volume fraction, spacing, average radius, etc., were determined by quantitative metallographic means. In this way the effects of controlled particle sizes and shapes on creep and tensile strengths could be studied over a wide range of particle spacings.

To actually assign a strengthening value to the different types of particles, a scheme was devised whereby the particle strengthening could be separated from the solid-solution strengthening. The strength of the alloy was considered to consist of essentially two main parts, that due to the matrix solid solution, and that due to the particle effects. By subtracting the matrix strength (determined from X-ray measurements of the matrix composition, and from single-phase strength curves) from the overall measured strength, the remainder could be ascribed to particle strengthening.

Curves of particle strengthening versus spacing were constructed for alloys with spherical and with platelike particles. The curves were strikingly different. For spherical particles, the particle-strengthening increment first decreased with increasing spacing to a critical spacing of about 50 microns. At larger spacings the strengthening increment rose, then tended to zero as infinitely large spacings were approached. For the platelets the particle strengthening rose directly with spacing, reached a maximum near 15 microns, then tapered off to zero. Greater strengthening appeared to be realizable with platelets than with spheres.

The curves obtained at room temperature with tensile tests were closely similar to those obtained with elevated-temperature creep tests. This observation is important because profuse stress-induced precipitation occurred during the high-temperature creep test, but not during the room-temperature tensile test. Thus, it was concluded that the effect of the initial particle distribution is apparently quite persistent.

The increase in strengthening with wider spacings may be due to an optimum interaction between particles and substructure boundaries which act similarly to precipitate particles in obstructing slip. Although the strengthening effect of grain and subgrain boundaries has been demonstrated before in other alloys, the evidence for these aluminum-copper alloys was not too conclusive. This is an important point and merits further investigation.

The relative strengthening of alloys with a small particle spacing versus those with a large spacing (less than 50 microns) were investigated over a range of stresses and temperatures. A reversal in strength was noted for the alloys in the intermediate stress range, whereby the alloy with coarser spacing became stronger. Of course, at room temperature (high stresses) the alloy with finer spacing was stronger. Also, at high temperatures (low stresses) the finer spacing appeared to give the higher strength. These findings corroborated the evidence previously submitted by Dorn and co-workers for aluminum-copper alloys with spherical particles. The alloys with platelets followed the same scheme, except that the reversals appeared to occur at slightly different

W  
1  
1  
9

stresses. The reasons underlying this behavior must be clarified completely before a sound theory of particle strengthening can be developed for high-temperature deformation.

The extension of these two years of research led to the present program, in which further work with particulate alloys was pursued. In particular, the effects of an applied stress on particle dissolution, grain growth, and precipitation were studied. These processes are only a few of the instabilities occurring in an alloy during creep. No theories of particle strengthening allow for such transient phenomena; furthermore, very little is known about the unstable processes in a quantitative way. It is hoped to augment the knowledge of the isolated processes sufficiently to permit an understanding of the more complex case when all variables operate simultaneously during creep.

## EQUIPMENT AND EXPERIMENTAL PROCEDURES

### Preparation of Specimens

Four alloys of 1, 2, 3, and 4 weight percent copper were prepared from 99.996 percent aluminum and 99.999 percent copper. The details of melting and fabrication have been recorded in references 2 and 3. Spectrographic and chemical analyses are listed in table I for the four sections of each ingot.

The bulk of the creep and tensile testing was performed on flat tensile specimens  $2 \frac{11}{16}$  inches long,  $\frac{9}{16}$  inch wide (at the shoulder) and  $\frac{1}{8}$  inch thick. The gage sections were 0.250 inch wide and 1 inch long. Other tests utilized specimens of the same dimensions as above, except the thickness was 0.090 inch.

Tensile specimens were heat-treated in salt pots to various initial grain sizes. In order to get a very fine initial grain size, an additional cold reduction and a lower recrystallization temperature was necessary. Details are given in table II.

Other specimens were overaged for 4 to 6 days at temperatures  $T_c$  where aging occurs most rapidly. Later, the particles were partially dissolved away at temperatures  $T_s$  just within the single-phase field. These temperatures are as follows:

Composition, weight percent, Cu	<u>1</u>	<u>2</u>	<u>3</u>	<u>4</u>
T <sub>c</sub> (C)	300	351	390	420
T <sub>s</sub> (C)	370	415	470	510

After heat treatment the specimens were electropolished in a glacial acetic acid and perchloric acid solution. Knoop indenter impressions were placed 1 inch apart on the gage section to facilitate strain measurements during creep.

### Creep Measurements

The creep equipment was housed in a constant-temperature room at  $26 \pm 1^\circ \text{C}$ . The furnace temperatures could be controlled within  $\pm 2^\circ \text{C}$ , and the temperature variation along the specimen was held to within  $\pm \frac{1}{2}^\circ \text{C}$ .

Direct loading was used almost exclusively, and the applied load was determined within 0.1 pound. Creep elongation was measured optically from outside the furnace with a sensitivity of about 50 microinches.

For a typical grain growth run under stress, perhaps six specimens would be used. A creep run lasting, say, 100 minutes would be made, then the load would be released and the specimen quenched into a water bath. Another specimen would then be crept under the same conditions to, say, 80 minutes, then quenched. Additional specimens might then be crept for 60, 40, 20, and 10 minutes. This procedure would give six specimens for metallographic inspection to determine the grain growth curve under stress. Approximately 8 minutes were required for the specimen to reach the desired temperature after the load was applied so the shorter times under stress were avoided as much as possible. Creep data are presented in table III.

### Tensile Tests

Room-temperature tensile tests were conducted at a strain rate of about 3.18 percent per minute. The specimens were held by yoke and pin adaptors and gripped at the shoulders, with the load being applied through a 9:1 lever arm. The stress was determined from a calibrated ring gage and the strain was read from a dial gage, which could be read to 0.0001 inch, attached to the upper extension arm. The tests were usually discontinued shortly after the maximum load was detected. Tensile data are recorded in table IV.

## X-ray Data

An X-ray diffraction examination was performed on filings from samples heat-treated to the desired condition. To avoid changes in the alloy, the filings could not be annealed prior to the X-ray exposure. Thus, some line broadening due to strains introduced by filing could not be avoided.

Lattice parameters were determined graphically from photographs obtained in a 114.59-mm Debye-Scherrer camera using unfiltered copper radiation. An estimate of the accuracy of the determinations is included in the summary of the X-ray data given in table V.

## Quantitative Metallography

The volume fraction of precipitate particles was measured under the microscope by means of lineal analysis, using a Hurlbut counter. The particle spacings were obtained concurrently by registering the number of particles intersecting random straight lines (many traverses) of known length.

Very fine precipitate, such as obtained during creep at elevated temperatures, was photographed at random, then a square grid of 20 lines per inch was superimposed on the print. In this case, point counting from photographs gave the volume fraction of the precipitate.

Grain sizes were measured from polished and etched, mounted specimens. The number of grain boundaries intersected by random straight lines (many traverses) of known length gave the mean diameter of the grains. These values can then be converted into the corresponding ASTM number by means of the table given on page 405 of reference 4, if desired. Grain size and particle data are assembled in tables VI to XI.

## EXPERIMENTAL RESULTS AND DISCUSSION

### General

Figure 1 sketches the aluminum-rich portion of the aluminum-copper phase diagram with which we are concerned. The various marked locations indicate the temperatures and compositions where experimental work was performed.

This investigation may conveniently be divided into three main parts. They are:

(1) Particle dissolution. The crosses in the single-phase region show where overaged alloys were held for various lengths of time to (a) Give a sequence of particle spacings, and (b) study particle dissolution, with and without an applied stress. Overaging was conducted at locations marked by triangles which represent temperatures where aging proceeds most rapidly.

(2) Grain growth. High-temperature, single-phase grain growth was studied both with and without an applied stress. Locations are marked by circles; the numbers to the left indicate stresses in psi.

(3) Two-phase creep. The solid square marks the temperature where overaged 3-percent-copper alloys were crept at 2,400 psi. Later, several specimens, interrupted successively from the creep run, were subjected to a detailed examination for grain growth, particle dissolution, and stress-induced precipitation.

Further details will be supplied in the discussions of these three main sections.

### Particle Dissolution

Particle dissolution without applied stress.- Precipitate particles were produced in aluminum alloys with 2, 3, and 4 percent copper by overaging at the critical temperatures recorded previously and indicated in figure 1. The results obtained with the 3-percent-copper alloy are shown in figure 2, in which the volume fraction of precipitate is plotted as a function of dissolution time at the temperatures noted. A semi-logarithmic plot is employed to indicate the approximate linearity obtained with the data for 500° C.

It will be noted that very small amounts of precipitate are involved at the higher temperatures or longer times. Thus, small deviations from sample to sample appear to give sizeable scatter. Actually, on a linear plot the points adhere rather closely to the best line. Another point to take into account here is the rapid drop in percent precipitate, even at times as short as one minute. Other runs at lower temperatures would be desirable to better chart the complete particle dissolution versus time curve. However, it is believed that adherence to the customary sigmoidal-shaped curve (ref. 5) was obtained because the data conform well to a kinetic analysis based on such a reaction curve.

W  
1  
1  
9

The data for dissolution of particles with time adhere adequately to an equation of the form

$$y = 1 - \exp(-t/k)^n \quad (1)$$

where  $y$  is the fraction dissolved in time  $t$ ,  $k$  is a temperature-dependent rate constant, and  $n$  is a constant. This type of equation has been applied successfully to many kinds of transformations that occur in metallic systems (refs. 5, 6, 7, and 8).

Results obtained by plotting the linear form of equation (1) (i.e.,  $\log\left(\log \frac{1}{1-y}\right)$  versus  $\log t$ ) are given in figure 3. The data points appear to fall fairly well along a straight line, except for one bad point obtained at 540° C, which also shows up in figure 2. A plot of the type employed in figure 3 is a sensitive test of the accuracy of the original data. Similar curves were obtained for dissolution of particles in alloys with 2 and 4 percent copper. The results obtained with an applied stress will be discussed later. In cases where equation (1) applies to nucleation and growth processes (ref. 8), the constants can be interpreted in terms of detailed mechanisms. Here, for particle dissolution the adherence of the data to equation (1) implies that the reverse process of disappearance and shrinkage of particles could also be analyzed similarly. However, the data are not extensive enough to justify these further calculations.

The curves of figure 2 were analyzed for the activation energy required for particle dissolution in 3-percent-copper alloys. The times required for 92 and 96 percent dissolution, at temperatures of 500°, 540°, and 570° C, yielded an activation energy of about 70 kcal/mol. This value is close to that obtained for grain growth in aluminum, and further comments will be made in the section on "Activation Energies."

The effect of temperature on the mean particle spacing curves of 3-percent-copper alloys is compared in figure 4. As dissolution proceeds, the spacings should get larger and ultimately approach infinity as the single-phase condition is reached. However, at the lower temperatures, the spacings hold relatively constant because the larger particles are quite persistent. In fact, they even become larger temporarily, due to a greater thermodynamic stability compared to small particles, then later dissolve away.

Particle dissolution under stress.— Curves of particle dissolution under stress are qualitatively similar to those shown for unstressed alloys in figure 2. For particulate alloys in a single-phase field, it was expected that the effect of stress would be to accelerate dissolution, but not to retard the dissolution. However, under a stress

of 200 psi more precipitate was found than in unstressed alloys at comparable times and at the higher temperatures. An increase in the amount of precipitate under stress has been observed before (refs. 3 and 9) but not in a single-phase field. Since particle dissolution was also proceeding under increasing creep strain, the latter was used as a variable to try to explain what was happening.

At the top of figure 5, the particle volume in 3-percent-copper alloys under a stress of 200 psi is plotted versus creep strain. Over the temperature range of  $500^{\circ}$  to  $570^{\circ}$  C, the data conform well to one curve drawn through all the points. The particle spacings for these alloys also follow the same pattern when plotted against strain. The implication in this strain dependence is that the amount of precipitate at any strain is a function of both the temperature and the time required to reach that strain. This type of functional dependence would then explain the apparently anomalous results mentioned above using time alone as the variable.

To test this idea it is necessary to demonstrate a time-temperature dependence of the dissolution process. The lower part of figure 5 shows the results obtained, without stress and with an applied stress of 200 psi, when the volume fraction of particles dissolved is plotted against  $T(C + \log t)$ , where  $T$  is the absolute temperature,  $t$  is the time, and  $C$  is a constant. If the volume fraction is a function of time and temperature in one case and a function of strain in another, then the strain must be some function of time and temperature.

At different stresses a family of curves similar to that given in figure 5 (upper) should exist, and these are shown in figure 6 for a temperature of  $500^{\circ}$  C. The volume of precipitate decreases sharply with the early strains, then levels off. The highest value for 800 psi is not necessarily due to experimental scatter, since particles below the limit of resolution could be detected after their coalescence. An interesting aspect of the three curves lies in their approximate constancy between strains of about 7 to 27 percent. At larger strains, of course, the amount of precipitate should decrease to zero; however, some kind of dynamic equilibrium appears to have been set up in which a conservation of precipitate volume is maintained. If this so-called "metastable precipitate level" is plotted against stress, the curve inserted within figure 6 ensues. This curve reveals that a critical stress of more than 200 psi is necessary to maintain this metastable condition. An inspection of the creep curves for stresses of 500 and 800 psi reveals that strains of 7 to 27 percent correspond to the region where viscous creep behavior predominates. Thus, the metastable precipitate level may be associated with a mechanism of stress-induced migration of vacancies believed to be operative during second-stage creep.

W  
1  
1  
9

If such is the case the features of the curves shown in figure 6 may be explained on the basis of two opposing tendencies. One is the tendency to dissolve particles by the interchange of solute atoms at the precipitate surface with vacancies, as proposed by Hyam and Nutting in reference 10. The other is the tendency to growth of preexistent voids by vacancy condensation (ref. 11). The steep drop in volume of precipitate at early strains corresponds to a high rate of generation of vacancies (i.e., a high creep rate). The leveling off results from a constant rate of generation of vacancies (steady creep rate), which condense preferentially at voids due to the difference in activation energies involved. When the creep rate increases in the third stage, sufficient vacancies are generated to satisfy both the growth of voids and the dissolution of particles, and the volume fraction of particles should decrease. The higher level of metastable precipitate at greater stresses can be explained in the same terms. The steady-state creep rate will be attained sooner at the higher stress, thus leaving more precipitate undissolved when the metastable precipitate period is reached. It appears that the brief explanation offered above can satisfactorily explain the observed behavior in terms of presently acceptable concepts; however, the explanation is qualitative and needs further exploration and verification before it can be said to rest on a firm foundation.

When the data for particle dissolution under stress are plotted as in figure 3, similar curves are obtained. A comparison of the curves for 3-percent-copper alloys, with and without stress, reveals no effect of stress at 500° C. However, at 540° and 570° C, the curves representing the stressed alloy lie below those for the unstressed state. The slopes also increase more with temperature for the stressed state, but detailed calculations appear unwarranted since the slopes are not too well defined. The effect of increased stress at constant temperature is merely to increase the level of the curves, for example, the slopes appear equal for stresses of 200, 500, and 800 psi at 500° C with overaged 3-percent-copper alloys.

Particle strengthening at room temperature.— The purpose of this phase of the investigation was to further test particle-strengthening effects in alloys with particle spacings near 50 microns. This critical spacing was found previously (ref. 2) to correspond to a minimum in the particle-strengthening curve for spherical particles. A finding of this nature was deemed important enough to be given further experimental verification.

As was described previously in the section entitled "Background," X-ray measurements gave the composition of the matrix; the strength of the single-phase alloy corresponding to this measured composition was determined from a suitable curve; and the particle-strengthening increment was then determined as the difference between the measured strength

and the matrix strength. Since the overall measured strength of the alloys includes all the strengthening effects associated with the particles, such as coherency strains, local composition gradients, interaction effects, and so forth, the proposed technique lumps all contributions to strengthening, other than matrix strengthening, under particle strengthening.

The plot in figure 7 includes the single-phase strength curve from which the matrix strengths were obtained. The data were collected from several sources, so the best values for the curve were determined from another plot that could account for variations in strain rate. It is seen that all overaged alloys are weaker than those given an additional 15 minutes dissolution treatment, and that the single-phase alloys are strongest. Thus, the tensile strengths of these overaged alloys rise as dissolution proceeds, then approach a level value. It is noteworthy that the same sequence of strength levels is found in these alloys when creep tested at 300° C under a stress of 2,400 psi (ref. 2). Evidence of this sort serves to emphasize the importance of the matrix-strengthening contribution in particulate alloys with large incoherent particles.

W  
1  
1  
9

The particle-strengthening curve (derived as described above) for spherical particles in aluminum-copper alloys at room temperature is shown in figure 8. Particle spacings extend out to about 540 microns; therefore, a broad range is covered. Qualitatively, the results are in accord with those obtained previously. At the smallest spacings there is the customary decrease in strengthening as the spacings widen. The critical spacing falls between 25 and 45 microns, and a sharp peak occurs at spacings near 75 microns. Thereafter, the strengthening increment decreases as the spacings become wider. At infinite spacing the alloy would consist of matrix only, and the particle-strengthening increment would become zero.

The discrepancies between the curve in figure 8 and the original curve obtained previously (ref. 2) are more apparent than real. The main difference lies in the sharp peak at 75 microns in figure 8 since this was not observed before. However, there were no data points between about 50 and 200 microns, so this new peak was missed entirely. On the whole, the old points and the new combine very satisfactorily about the new curve given in figure 8, except that the critical spacing is probably between 25 and 45 microns.

Of course, the major question raised by this particle-strengthening curve concerns the reason for the large strengthening increase near 75 microns. It is axiomatic in almost all theories of strength that the strength of alloys increases as the particle spacings become finer. Between the critical and the peak spacings, however, the strengthening increment increases. Previous experimental work upon which theory is

based failed to show an upswing in strength, probably because the critical spacing was not exceeded. Another point is that no effective attempts were made to separate solution-strengthening effects from particle-strengthening effects. Yet, it is inevitable (e.g., during tempering of carbides in plain carbon steel) that the concentration of the matrix varies as the particle sizes and spacings are modified.

W  
1  
1  
9  
The role of structural features other than particles must also be reexamined from the standpoint of their ability to obstruct slip. For example, the efficacy of the grain boundary as an obstacle to slip has been demonstrated in several investigations. Hall (ref. 12) has proposed a quantitative relationship between hardness and the grain diameter. In reference 13 it was shown that tensile strength versus particle spacing in steels does not correlate linearly until grain boundaries are included in the count with particles. In reference 14 both inclusions and grain boundaries were counted to obtain a "spacing" in ferrite. Furthermore, Ball (ref. 15) has demonstrated an increase in the flow stress of aluminum with decreasing size of the subgrains. Significantly enough his relationship has the same form as that suggested by Hall, that is, strength (or hardness) varies inversely as the square root of the subgrain (or grain) size. Finally, Hyam and Nutting (ref. 10) concluded that the hardness of tempered plain carbon steels depended on the ferrite grain size.

On the basis of evidence such as has been advanced above, it seems that boundaries have appreciable strengthening potentialities. Thus, it is possible that the increased strengthening effect found in aluminum-copper alloys with particle spacings near 75 microns can be explained by the presence of subgrains. Subgrains were not specifically identified, although an unusual "lineage" effect on a subgranular scale was noted in overaged, solution-treated, and etched<sup>1</sup> alloys of aluminum with 1 to 4 percent copper. The effect consisted of a pattern of lines, the density of which increased with the copper content, characterized by a remarkable straightness, broken only by abrupt 90° turns as they zig-zagged away from the grain boundaries and particle interfaces.

If subgrains are responsible for these patterns, then increased subgrain formation results from particle dissolution since the copper content in the matrix increases. With the optimum combination of particle spacings and subgrain size, a maximum in strengthening is achieved. As the particle spacings increase, the curve falls off, and finally, if subgrains are all that remain, a positive strengthening value should persist even at infinite particle spacing. These possibilities have not been investigated systematically yet, but it will be necessary before more definite conclusions can be drawn.

---

<sup>1</sup>About 4 hours in a xylene solution.

An alternative to the idea proposed above is suggested by the dissolution method used to obtain the various particle spacings. It is possible that a wave of copper atoms diffusing outwardly from the particles creates a larger spherical volume with a relatively high copper content. This is suggested by a few fuzzy halos observed in etched alloys around the partially dissolved particles. Increased strengthening might then be obtained by a greater volume of strained material, or by the decreased free path between these high-copper volumes. However, the particle spacings in these cases were so enormous, relatively speaking, that it is hard to conceive of any significant decrease in the interparticle path by this process. Furthermore, both X-ray and electron-microscope evidence (ref. 2) denied the presence of such concentration gradients as well as submicroscopic particles. Therefore, at the present stage of the investigation, the subgrain idea appears more acceptable. The reality of the strengthening peak at 75 microns does seem to be established; what remains to be done is to demonstrate the reasons for its existence. Those cases reported in the literature where the coarser particle spacing was associated with a stronger alloy may be due to the increase in strengthening between the critical and peak spacings.

### Grain Growth

Grain growth without applied stress.—Reference to figure 1 reveals the temperatures where isothermal grain growth was studied in aluminum-copper alloys with 1, 2, 3, and 4 percent copper. The temperatures extended from 420° to 580° C for the alloys and from 350° to 600° C for pure aluminum (ref. 16). The data for aluminum are not strictly applicable to the present study because the starting material was the cold-rolled alloy. Here, the alloys were first heat-treated to a definite grain size. In this way the time variable applies only to time for grain growth and does not include an incubation time, recrystallization time, or the growth time necessary to get the initial grain size. Details of the preliminary heat treatments used to obtain the desired initial grain sizes have been given in table II. For convenience, the data for grain growth without an applied stress will be considered first, then the results for grain growth with stress.

Satisfactory linear plots were usually obtained with the grain-growth data when  $\log$  (grain diameter) was plotted versus  $\log$  (growth time). Examples of the compositional variation of grain growth in aluminum-copper alloys at 540° C are offered in figure 9, and the temperature dependence of grain growth in 2-percent-copper alloys is given in figure 10. In figure 9 the data points are plotted only for the 3-percent-copper alloys because of the closeness of the other curves. The scatter of points about the straight line is representative of that for the other alloys, however.

A straight line fits the data points for these alloys satisfactorily over a 3- or 4-cycle range in time. Thus, the equation proposed by Beck et al. (ref. 16),

$$D = kt^n \quad (2)$$

where  $D$  is the average grain diameter,  $t$  is the time, and  $k$  and  $n$  are constants, appears to describe the data. The definition of the time, as used here, differs from the convention adopted by Beck et al., in that it represents time for grain growth only.

The slopes of the grain-growth curves  $n$  are plotted versus reciprocal temperature in figure 11. The curves approach linearity at the lower temperatures but seem to curve downward at higher temperatures. Only in the case of the 4-percent-copper alloy, at its solidus temperature, does the value of  $n$  closely approach  $\frac{1}{2}$ . The number  $\frac{1}{2}$  was derived by Beck et al. on the basis that the grain-boundary energy is responsible for grain growth. It is obvious that other factors are operative, and these have been discussed to some extent by Burke and Turnbull (ref. 17).

The nonuniform position of the curve for the 2-percent-copper alloys represents a retardation of growth rates over a wide temperature range. This can be seen more clearly in the "contour" plot constructed in figure 12. Curves of equal  $n$ -values are plotted in the aluminum-rich portion of the aluminum-copper phase diagram. Concave downward bulges appear in the vicinity of the 2-percent-copper composition and break the smooth continuity of the curves. It can be seen that these bulges correspond to a retardation of growth rate because, for the same  $n$ -value, a relatively higher temperature is necessary for 2-percent-copper alloys than for adjacent alloys.

This behavior is believed to be related to other abnormal strengthening and retardation effects observed in this system near 2 percent copper. An area of retarded age hardening was described in the "Background" for 2-percent-copper alloys near 300° C. The relative creep resistance in alloys undergoing precipitation at this composition and temperature was also greater. An increase in the room-temperature tensile strengths are shown for quenched 2-percent-copper alloys in figure 7. Figures 9, 11, and 12 also reveal anomalous grain-growth behavior in the same alloy in the single-phase region. These observations may now be rationalized to some extent. In general, retardation of the rate of a reaction may be due to either a lower rate of nucleation or a lower rate of growth, or both. On the basis of what is now known, it is believed that the rate of growth is responsible for the retardation effects in alloys with compositions near 2 percent copper. The first item of evidence to this effect is that the particle spacings in overaged 2-percent-copper alloys are less than in overaged 1-, 3-, or 4-percent-copper alloys

(ref. 2). A smaller particle spacing is associated with more numerous particles, so the rate of nucleation is greater, if anything, than in the other alloys. Thus, a relatively slower rate of growth must be the overall rate-determining factor. The other item concerns the growth rates in aluminum-copper alloys in the single-phase region. Here, it is shown directly that the 2-percent-copper alloys exhibit a marked retardation in growth rates relative to the other alloys.

For the processes of two-phase precipitation and single-phase grain growth, it seems credible that the retardation in rates is due to a relative decrease in the rate of growth. If growth in both cases is dependent on the movement of vacancies, this would require an activation energy for self-diffusion. Hyam and Nutting, reference 10, have presented some support for this idea in the case of particle growth and grain growth in plain carbon steels. Activation energies for both processes in aluminum-copper alloys also appear to fit this explanation, but difficulties in defining the activation energy cloud the issue. This matter will be discussed more thoroughly later.

Another possibility for explaining the anomalous effects in alloys near 2 percent copper (about 0.86 atomic percent copper) is that compound or ordering tendencies are present. For an alloy with a composition of 0.833 atomic percent copper, a combination of 1 copper atom with 119 aluminum atoms is required. Compound formation in such dilute concentrations is virtually unknown, so perhaps ordering tendencies are operative. Many unusual effects have been noted in single-phase alloys (refs. 18 and 19) so this possibility must not be completely discounted.

In a study of the rates of precipitation in gold-nickel alloys (ref. 8), areas of retardation similar to those reported here were found. The diffusion (ref. 20) and thermodynamic (ref. 21) properties were also available for this system. A drastic decrease in the diffusion rates was related to the lower thermodynamic driving force for diffusion which, in turn, coincided with the areas of retardation for precipitation and precipitate growth. The importance of such findings to the present study lies in the possibility of explaining and understanding these retardation phenomena, especially with regard to the enhanced creep properties that are obtained.

Returning to figure 11, if the  $n$ -values are plotted for the various alloys at constant temperature, a smoothly ascending curve is obtained except for a dip at the 2-percent-copper alloy. A similar dip in  $n$ -values can be seen in the grain-growth data for an aluminum alloy with about 0.7 percent manganese, investigated by Beck, Holzworth, and Sperry (ref. 22); however, no such effect is found by Demer and Beck (ref. 23) in alloys of aluminum with up to 2 percent magnesium. It would be extremely interesting from the standpoint of the ideas discussed above if the strength of these alloys were known. Additional experimental

confirmation of a relationship between areas of retardation and an increase in strength properties is highly desirable from both a theoretical and practical point of view.

Variations in initial grain size.- In order to gain some insight into the effects of initial grain size on subsequent grain growth, grain sizes of ASTM -3, +1, and +3 were produced in 3-percent-copper alloys.<sup>2</sup> Details of the heat treatments have been given in table II. Growth runs were made at 500°, 540°, and 570° C, and conformity to linear behavior was found similar to that depicted in figure 10. Also, the slopes increased regularly with increasing temperature for any one initial grain size.

When the grain-growth curves are compared at the same temperature, a direct sequence with the initial grain sizes is not obtained. The curves presented in figure 13 show the large grain size of the -3 alloys essentially unchanged, the +1 alloys having the steepest slope, and the +3 alloys occupying an intermediate position. Since the thickness of the +3 alloy sheet was only 0.090 inch, compared with 0.125 inch for the other alloys, it was thought that the "specimen-thickness effect" demonstrated by Beck et al. (ref. 16) may have been operative here. However, this effect does not seem applicable because no flattening of the +3 alloy curve was noted, and because the largest grain sizes attained were well below the sheet thickness. Rather, it would appear that the -3 alloys were the nonconformists, and that longer times or higher temperatures were needed, even though the grain size was about one-half the thickness of the sheet. Nevertheless, it should be noted that the slopes vary inversely with the grain size at some intermediate time.

Since the -3 alloys are so insensitive over the growth times and temperatures investigated, only the +1 and +3 alloys will be compared. In all cases, the curves for the +3 alloy lie well above the curves for the +1 alloy, as would be expected. On the other hand, the +1 alloys have steeper slopes than the +3 alloys. This rather unexpected behavior can very possibly be traced to differences in the incubation times necessary for grain growth to start. A linear extrapolation of the growth curves back to the initial grain sizes gives about 0.1 minute for the +3 alloy and about 3 minutes for the +1 alloy. When grain growth finally starts in the +1 alloys, the grain size is much smaller than that already reached in the +3 alloys, so the growth rate is greater. These findings point up the need for considering both the incubation time as well as the growth rate, when deciding on the maximum grain size allowable in an alloy.

From a practical standpoint, the findings may be summarized as follows: (1) In alloys with a very large initial grain size (ASTM -3) no

---

<sup>2</sup>For convenience, these alloys will be referred to hereafter as -3, +1, or +3 alloys, respectively.

appreciable grain growth occurred during a 200-minute period, even at temperatures up to about 20° C below the solidus; (2) in alloys with a medium-large initial grain size (ASTM +1) the grain size during grain growth was less and the growth rate was greater than in alloys with a finer grain size; (3) in alloys with a very fine initial grain size (ASTM +3) rapid grain growth occurred at early times, then growth proceeded at a rate more typical of a larger grain size; (4) an incubation period for grain growth was greater, the larger the initial grain size.

Grain growth in particulate alloys.— The bottom curve in figure 13, labeled "Overaged," depicts grain growth at 500° C in an alloy that was heavily overaged before testing. The data points for the two-phase alloys are also described by a straight line. The initial grain size was very small, about 0.03-mm diameter. An interesting point here is that the slope of the grain-growth curve is nearly the same as the +1 alloy curve. In an alloy with particles, the rate of grain growth would be expected to be less than that in a solid solution, even at temperatures in the single-phase region.

W  
1  
1  
9

The linear increase in grain size (on log-log coordinates) is somewhat surprising because over half the precipitate is dissolved within the first minute (see fig. 2) and a linear rate of dissolution is not achieved until after 10 minutes. Furthermore, the particle spacings rise quite gradually up to 70 minutes, then increase drastically (see fig. 4). The particle radius  $r$  was computed for these alloys by an expression due to Fullman (ref. 24) for uniform spherical particles. It is

$$r = \frac{3}{4} \frac{f_v}{N_L} \quad (3)$$

where  $f_v$  is the volume fraction of particles, and  $N_L$  is the number of particles intersected per millimeter by a straight line. A sharp upward break was also obtained at 70 minutes when  $r$  was plotted versus time. Apparently, the increase in spacing and increase in particle radius are so proportioned that a steady rate of dissolution results (after 10 minutes). Based on this evidence, it is suggested that the grain size is inversely related to the volume of precipitate (after 10 minutes) rather than to the particle radius or spacing.

At early dissolution times (less than 10 minutes), the grain size appears to be controlled by the particle radius, in line with a suggestion of Zener's, quoted by Smith (ref. 25). Based on grain-boundary energy considerations, he derived the expression

$$R \cong \frac{3}{4} \frac{r}{f_v} \quad (4)$$

relating  $R$  the radius of the grain to  $r$  the radius of the particle, and  $f_v$  the volume fraction of particles. Adherence to the approximate

equality expressed in equation (4) was obtained only for times up to 10 minutes but with a slope of about  $\frac{3}{7}$ . At greater times the grain size gradually became less than that predicted by Zener's relationship. Apparently, equation (4) is valid only for grain growth in the presence of smaller particles (up to 10 minutes) and under conditions of greater particle stability.

In addition to the experiment described above, that is, grain growth in an overaged alloy in the single-phase region, a study was made of grain growth in a single-phase alloy at a temperature within the two-phase region. Single-phase alloys of 3 percent copper were held at 460° C for times up to 460 minutes, but during this period no detectable grain growth occurred. Even though this temperature is only about 5° C below the solvus temperature, an increasing amount of precipitate was seen, both within the grains and along the grain boundaries. Beck et al. (ref. 22), studied the effects of particles in aluminum-manganese alloys on grain growth and reported a complete cessation of growth at temperatures just below the solvus. It appears immaterial, for the case of grain growth within the two-phase field, whether particles are present initially or not since grain growth is inhibited in either case. This behavior shows that the effectiveness of the very early precipitate in inhibiting grain growth is on a par with that of overaged particles.

Grain growth under stress.- A study of the effects of an applied stress on grain growth was also undertaken. Figure 1 documents the compositions, temperatures, and stresses involved. An initial grain size of ASTM +1 was employed for all alloys, with additional grain sizes of ASTM -3 and +3 for the 3-percent-copper alloys. Thus, two additional variables, stress and initial grain size, are added to composition, temperature, and growth rate.

Figure 14 summarizes much of the grain-growth data obtained with an applied stress. In the plot on the left, the slope  $n$  is plotted versus applied stress, with two variables held constant. On the right, the slope  $n$  is plotted versus temperature, with only composition held constant. The plot at the left shows that the effect of an applied stress, for all compositions, is to raise the value of  $n$ . The curve for aluminum is unknown, however, a rapid increase would be expected. At zero stress the rate increases linearly with composition, except for a dip at 2 percent copper. At 200 psi there is also a minimum in rate at 2 percent copper. Various aspects of this retardation behavior have been discussed previously for unstressed alloys. The effect seems to persist even in the presence of an applied stress. The average increase in growth rate with stress decreases regularly with increasing copper content of the alloys; that is, the applied stress increases the growth rate less in the stronger alloys. There is also a hint that some curves

are flattening out, so stresses greater than 200 psi may not cause appreciable change in growth rates.

The effects of temperature on the slope  $n$  are shown at the right, for stresses of 0 and 200 psi, and for the three initial grain sizes. In all three cases the effect of temperature is to increase the  $n$ -values; the effect of stress is to raise the level of the unstressed alloy curve. Here again, as for the unstressed alloys, the +1 alloys have the highest values of  $n$ , and the +3 alloys fall in the intermediate position. Apparently, the applied stress does not alter the relative length of the incubation periods. The effect of stress on the temperature dependence of  $n$  is very slight for the -3 alloys, a little greater for the +3 alloys, and greatest for the +1 alloys. This observation may be summarized by the statement that the temperature dependence of the growth slope  $n$  varies directly with the magnitude of  $n$ . This finding is of interest because it indicates that the initial grain size may not always be the best criterion for certain aspects of elevated-temperature performance.

Activation energies.- Various attempts were made to determine the activation energies involved in the grain growth of these alloys. Just as Beck, Holzworth, and Hu (ref. 26) found with aluminum, no unique activation energy could be determined for the alloys, because the temperature dependence of the true growth rate ( $dD/dt$ ) varies with the grain size. Thus, depending on the grain size selected, different values of activation energy are obtained. For example, in aluminum, the activation energy determined at a grain size of 0.5 mm equals about 60 kcal/mol, and for a grain size of 1.0 mm the activation energy is roughly 80 kcal/mol.

Curves of true growth rate versus grain diameter are plotted for 2-percent-copper alloys at various temperatures in figure 15. The data are described fairly well by straight lines, and the change in slope with temperature agrees qualitatively with the behavior noted by Beck et al. (ref. 26), for aluminum. A plot of this type also serves to check the validity of equation (2), since it predicts a linear variation of  $\log(dD/dt)$  and  $\log(D)$ , as indicated by the equation in figure 15. Beck et al., have used such curves to point out the dependence of the true growth rate on the instantaneous grain size. On the other hand, it can also be said that the true growth rate depends on the growth time, since equation (2) can be rearranged to give the equation entered in figure 16. A linear relation is predicted between  $\log(dD/dt)$  and  $\log(t)$  and does occur, as demonstrated by the plot in figure 16. The question of whether the latter curve can be used to obtain a more meaningful activation energy is brought up later.

The validity of equation (2) for describing grain growth appears to be well established, yet there are some aspects of the growth process which have not been examined. The reasons for the lack of parallelism

W  
1  
1  
9

among the curves of figure 15, and among similar curves for aluminum, for example, are unknown. Burke and Turnbull (ref. 17) noted that the activation energy for recrystallization of aluminum decreased at higher temperatures and the same observation can be made for grain growth. On the other hand, in 70-30 brass (ref. 27), the lines are parallel over a wide temperature range, so a unique value of activation energy can be obtained. It is possible that unique activation energies are obtained only at temperatures below about one-half of the melting point. A factor of about  $\frac{1}{2}$  usually gives the temperature separating low-temperature from high-temperature behavior. However, this factor is somewhat lower for pure metals and somewhat higher for alloys. This line of reasoning may explain why an activation energy can be obtained in 70-30 brass at temperature approaching 700° C, and no unique activation energy for aluminum at temperatures above 350° C.

Since the growth process is dependent on both time and temperature, it is logical to apply a function of time and temperature to growth data. Time-temperature parameters obtained by rearranging the Arrhenius rate expression have been used rather successfully for grain growth (refs. 28 and 29). The form of parameter  $P$  employed here is

$$P = T(C + \log t) \quad (5)$$

where  $T$  is the absolute temperature,  $t$  is the time, and  $C$  is a constant. The same function was used previously for describing particle dissolution (see fig. 5). Instead of arbitrarily selecting a constant value for  $C$  (e.g., 20) the best value for each alloy was determined from the data. This procedure has been shown to possess considerable merit in other applications (ref. 30) as well. A further advantage of this kind of plot is that data obtained over a wide range of times and temperatures can be reduced to a single curve. This procedure reveals the relative accuracy of the data, and permits a more reliable activation energy to be computed.

Activation energies for grain growth were computed from the parameter plots for aluminum and the four alloys with copper. Since the parameter values, and thus the activation energies, vary with grain size, the same ambiguity arises as mentioned before. However, for comparative purposes, activation energies for a grain size of 0.5 mm are plotted versus composition in figure 17. The latter values (dashed line) and those from true growth-rate plots (solid line) agree qualitatively with each other. A maximum in activation energy occurs at 3 percent copper, and a minimum at 1 percent copper, with the highest value for aluminum. This large value of activation energy for grain growth in aluminum is puzzling, although a temperature dependence of the activation energy for recrystallization in aluminum was noted (ref. 17). A value more closely approaching the activation energy for self-diffusion, about 33 kcal/mol, would be

expected. Several other values of activation energy are indicated for aluminum. These include Burke and Turnbull's value of 87 kcal/mol (ref. 17) reportedly obtained from reference 16. The latter gave a value of about 60 kcal/mol for a grain size of 0.5 mm, while a further calculation with their data gave an activation energy of about 80 kcal/mol for a grain size of 1.0 mm. About 78 kcal/mol was obtained by using the time required to obtain a grain size of 0.3 mm. This wide range of values indicates the vagueness associated with the term "activation energy" for grain growth in aluminum.

The points marked along the 3-percent-copper ordinate include the activation energies for grain growth under a stress of 200 psi. These values represent about a 40 to 50 percent reduction of the activation energies for grain growth without stress. The two solid circles represent activation energies for particle dissolution at stresses of zero and 200 psi, from the time for 96 percent dissolution. An applied stress of 200 psi decreases the activation energy for dissolution from 70 to 40 kcal/mol, which is about the same decrease experienced in the activation energies for grain growth. It is noteworthy that the activation energy of 66.5 kcal/mol for particle dissolution is so close to the 68 kcal/mol recorded for grain growth in aluminum (both obtained from parameter plots). This coincidence lends credence to the postulate (ref. 10) that grain growth and particle dissolution are both governed by the same process, and thus that the activation energies are equal. Unfortunately, only relative values are involved here, so further connection with the activation energy for self-diffusion in aluminum is not possible.

A major inconsistency with the previous results appears in the two curves of relative activation energy in figure 17. The retardation effects discussed before with the 2-percent-copper alloys would require a relatively high activation energy. In these curves, the activation energy for 2 percent copper is relatively low. Looking into this matter a little more closely resulted in the dot-dash curve depicted at the bottom of figure 17. The activation energies calculated there were obtained from the slopes  $n$  of the grain-growth curves. Since  $n$  does not have the dimensions of a rate, it is not strictly correct to call the temperature dependence of its slope an activation energy. However, the  $n$ -values are probably more indicative of the true relative grain-growth behavior than other parameters which are calculated from them. Figure 9, for example, reveals that the slope of the grain-growth curve for 2-percent-copper alloys is lower than would be expected. From figure 11 it can be seen that the slope of the 2-percent-copper alloy curve is also out of line. The trends from these data are reflected in the lowest curve shown in figure 17. Now, the 2-percent-copper alloys possess the largest activation energy (based on the upper limit of the experimental scatter). This curve is felt to be more representative of the true state of affairs than the other two activation-energy curves. It

may be appropriate at this time to suggest a new method for calculating activation energies, since the results appear to fit in with the lowest curve. Activation energies based on the time for a constant true growth rate (instead of being based on the true growth rate at some constant grain size), may eliminate some of the ambiguities noted in the other methods of calculation.

### Precipitation and Grain Growth During Creep

W In order to investigate the combined processes of grain growth,  
1 particle dissolution, and precipitation under stress, exploratory tests  
1 were conducted with overaged 3-percent-copper specimens at 300° C and  
9 2,400 psi. Interrupted creep tests gave five specimens crept to suc-  
cessively longer times before the load was released and the specimens  
were water quenched. The pertinent data are depicted graphically in  
figure 18. Since individual specimens were used for each point along  
the creep curve, an effort was made to insure their uniformity before  
testing. Creep strains, grain sizes, and heating-rate curves were  
obtained, as well as the volume fraction of precipitate. The variation  
in amount of both the coarse and the fine precipitate was measured by  
lineal analysis, and the particle density was obtained by counting par-  
ticles per unit area.

The course of the measured grain-size curve is qualitatively a  
mirror image of the total volume of precipitate curve. A similar con-  
nection between grain size and volume of precipitate was noted previously  
in the case of grain growth in a particulate alloy. Grain sizes were  
calculated according to Zener's expression (eq. (4)), using particle  
radii computed from the equations of Fullman (eq. (3)). A surprisingly  
good correspondence between the measured and calculated grain sizes is  
obtained, considering the various simplifications inherent in the calcula-  
tions. On the basis of these limited data, it appears that Zener's anal-  
ysis of the important factors governing grain growth in particulate alloys  
is essentially correct. The generality of equation (4), in that it does  
not appear dependent on changes in composition, particle spacings, dis-  
tributions, strain, etc., should help considerably to simplify a complex  
state of affairs.

The curve for total volume of precipitate versus time appears strange  
at first glance, but may be rationalized by consideration of the processes  
taking place during creep. The first tendency in these overaged alloys  
is to increase the volume of precipitate because the equilibrium amount  
is greater at the lower test temperature. An increase in the amount of  
precipitate would be expected for another reason. As Hyam and Nutting  
have shown quantitatively in figure 10 of reference 10, the larger par-  
ticles increase in size and the smaller particles decrease at early tem-  
pering times. Thus, fine particles originally below the limit of

resolution of the optical equipment can be measured when reprecipitated on the larger particles, and the volume fraction appears to increase.

Furthermore, this same tendency for smaller particles to dissolve and the larger particles to get larger is reflected in the behavior shown at 10 minutes. During further creep, readjustments in the precipitate gradually result in an approach to a steady-state condition - at least during secondary creep. As the third stage of creep is entered, however, this balance may be disturbed in such a way that the amount of precipitate rises. The increase in amount of precipitate at 45 minutes is not too unreasonable an event, especially if the stress is increasing as is the case in a constant-load test. This state of affairs may be due to either stress-induced precipitation in amounts greater than predicted by the phase diagram (ref. 3), or to the increase associated with higher stress which was shown previously (see fig. 6).

The validity of the above line of reasoning should be subjected to further experimental testing at different temperatures and stresses. Further work might be designed to prove or disprove theoretical analyses of the effects of stress on diffusion and deformation in metals, such as was offered by Hillert, reference 31. Clarification of the complex situation arising in particulate alloys during high-temperature creep should be possible. The close agreement obtained between the theoretical and measured grain sizes is an encouraging step in this direction.

## RÉSUMÉ AND CONCLUSIONS

### Particle Dissolution

The kinetic expression  $y = 1 - \exp(-t/k)^n$  where  $y$  is the fraction dissolved,  $t$  is the time,  $k$  and  $n$  are constants, describes the course of dissolution in overaged alloys of aluminum and copper, either with or without an applied stress. The activation energy for dissolution in 3-percent-copper alloys decreases from 70 kcal/mol without stress to 40 kcal/mol for a stress of 200 psi.

More precipitate was found at equal times with an applied stress than without. An analysis of dissolution as a function of strain indicated that the fraction dissolved depended primarily on the strain, rather than on the individual times or temperatures involved in reaching that strain. The implication of this strain dependence is that the amount of precipitate at any strain is a function of both the time and temperature required to reach that strain.

During strains corresponding to viscous creep behavior, a metastable level of precipitate is maintained; also, the greater the stress, the

W  
1  
1  
9

more the amount of precipitate. A tentative explanation of this behavior is advanced which appears to account for the important features of these curves. It is based on two competing processes, the dissolution of particles by a vacancy mechanism, and the growth of voids by the precipitation of vacancies.

The particle-strengthening increment due to spherical particles is seen to give a maximum at spacings near 75 microns, and a minimum near 35 microns. An optimum combination of subgrain size and particle spacings is believed to account for the peak found near 75 microns.

### Grain Growth

The equation proposed for grain growth by Beck et al. (ref. 16),  $D = kt^n$ , where  $D$  is the grain diameter,  $t$  is the time, and  $k$  and  $n$  are constants, satisfactorily applies to grain growth with or without an applied stress. Relative activation energies for grain growth decrease from about 60 kcal/mol without stress to about 30 kcal/mol for a stress of 200 psi in 3-percent-copper alloys. The effect of stress, and of temperature, is to increase  $n$ , the slope of the grain growth curve,

The relative activation energy for grain growth in aluminum is close to that for particle dissolution in 3-percent-copper alloys, suggesting that both processes are governed by the same rate-controlling process. The ambiguity in activation energies found with these alloys prevents evaluation of the vacancy mechanism suggested by Hyam and Nutting (ref. 10).

Contours of equal  $n$ -values, when superimposed on the phase diagram, reveal a retardation of growth rates in 2-percent-copper alloys. This corresponds with a previously determined retardation in the rate of age hardening and a relative increase in creep resistance. The behavior is attributed to a decreased growth rate of particles both during age hardening without stress and precipitation under creep conditions.

The effects of initial grain size on grain growth were examined in 3-percent-copper alloys annealed to a very large, a medium, and a fine grain size. Even up to 20° below the solidus, no appreciable grain growth occurred in alloys with the very large grain size. A greater grain size, but lower growth rate was obtained in the alloys with very fine grain size, compared to the alloy with a medium grain size. A difference in incubation periods before growth appears to be responsible for the latter behavior.

## Precipitation and Grain Growth During Creep

Overaged aluminum 3-percent-copper alloys were crept at 300° C and 2,400 psi. Lineal analysis gave the volume of both fine and coarse precipitate, and the grain sizes and creep strains were also obtained. At early times, the volume of smaller particles decreased while that of the larger particles increased. The volume of both the large and small precipitates increased at longer times and larger strains in accordance with the trend expected at higher stresses. Using calculated particle radii, grain sizes were computed according to Zener's expression relating particle radius and grain size. Close agreement was obtained between the theoretical and measured grain sizes in these alloys undergoing creep, precipitation, and grain growth.

W  
1  
1  
9

Battelle Memorial Institute,  
Columbus, Ohio, August 15, 1958.

## REFERENCES

1. Anon.: Relation of Properties to Microstructure. David Turnbull, Seminar Coordinator, ASM (Cleveland, Ohio), 1954.
2. Underwood, E. E., Marsh, L. L., and Manning, G. K.: Effect of Precipitate Particles on Creep of Aluminum-Copper Alloys During Age Hardening. NACA TN 4372, 1958.
3. Underwood, E. E., Marsh, L. L., and Manning, G. K.: Creep of Aluminum-Copper Alloys During Age Hardening. NACA TN 4036, 1958.
4. Anon.: Metals Handbook. ASM (Cleveland, Ohio), 1948.
5. Owen, W. S., and Wilcock, J.: Reactions Involved in the First-Stage Graphitization of Iron-Carbon-Silicon Alloys. Jour. Iron and Steel Inst., vol. 182, pt. 1, Jan. 1956, pp. 38-43.
6. Averbach, B. L., and Cohen, M.: The Isothermal Decomposition of Martensite and Retained Austenite. Trans. ASM, vol. 41, 1949, pp. 1024-1060.
7. Roberts, C. S., Averbach, B. L., and Cohen, M.: The Mechanism and Kinetics of the First Stage of Tempering. Trans. ASM, vol. 45, 1953, pp. 576-604.
8. Underwood, E. E.: Precipitation in Gold-Nickel Alloys. Sc.D. Thesis, M.I.T., 1954.
9. Roberts, C. S.: Interaction of Precipitation and Creep in Mg-Al Alloys. Trans. AIME, vol. 206, 1956, pp. 146-148.
10. Hyam, E. D., and Nutting, J.: Tempering of Plain Carbon Steels. Jour. Iron and Steel Inst., vol. 184, pt. 2, Oct. 1956, pp. 148-165.
11. Machlin, E. S.: Creep-Rupture by Vacancy Condensation. Trans. AIME, vol. 206, 1956, pp. 106-111.
12. Hall, E. O.: Variation of Hardness of Metals With Grain Size. Nature, vol. 173, no. 4411, May 15, 1954, pp. 948-949.
13. Turkalo, A. M., and Low, J. R., Jr.: The Effect of Carbide Dispersion on the Strength of Tempered Martensite. Trans. AIME, vol. 212, 1958, pp. 750-758.

14. Roberts, C. S., Carruthers, R. C., and Averbach, B. L.: The Initiation of Plastic Strain in Plain Carbon Steels. Trans. ASM, vol. 44, 1952, pp. 1150-1157.
15. Ball, C. J.: The Nature and Effect of Substructure in Polycrystalline Aluminum. Dislocations and Mechanical Properties of Crystals, J. C. Fisher, ed., John Wiley & Sons, Inc., 1957, pp. 353-358.
16. Beck, P. A., Kremer, J. C., Demer, L. J., and Holzworth, M. L.: Grain Growth in High-Purity Aluminum and in Aluminum-Magnesium Alloy. Trans. AIME, vol. 175, 1948, pp. 372-400.
17. Burke, J. W., and Turnbull, D.: Recrystallization and Grain Growth. Vol. 3 of Progress in Metal Physics, B. Chalmers, ed., Pergamon Press Ltd. (London), 1952, pp. 220-292.
18. Kornilov, I. I.: Creep of Solid Solutions and Compounds in Metallic Systems. Symposium on Creep and Fracture of Metals at High Temperatures (May 31-June 2, 1954), Nat. Phys. Lab. (London), 1956, pp. 215-219.
19. Goldschmidt, H. J.: Sigma-Phase Nucleation and Other Transformations During Diffusion in the Iron-Chromium System. Symposium on The Mechanism of Phase Transformations in Metals, Monograph and Rep. Ser. No. 18, Inst. of Met., AIME, 1955, pp. 105-119.
20. Reynolds, J. E., Averbach, B. L., and Cohen, M.: Self-Diffusion and Interdiffusion in Gold-Nickel Alloys. Acta Met., vol. 5, 1957, pp. 29-40.
21. Seigle, L. L., Cohen, M., and Averbach, B. L.: Thermodynamic Properties of Solid Nickel-Gold Alloys. Trans. AIME, vol. 194, 1952, pp. 1320-1327.
22. Beck, P. A., Holzworth, M. L., and Sperry, P. R.: Effect of a Dispersed Phase on Grain Growth in Al-Mn Alloys. Trans. AIME, vol. 180, 1949, pp. 163-192.
23. Demer, L. J., and Beck, P. A.: Effect of Composition on Grain Growth in Aluminum-Magnesium Solid Solutions. Trans. AIME, vol. 180, 1949, pp. 147-162.
24. Fullman, R. L.: Measurement of Particle Sizes in Opaque Bodies. Trans. AIME, vol. 197, 1953, pp. 447-452.
25. Smith, C. S.: Grains, Phases and Interfaces: An Interpretation of Microstructure. Trans. AIME, vol. 175, 1948, pp. 15-51.

26. Beck, P. A., Holzworth, M. L., and Hu, H.: Instantaneous Rates of Grain Growth. Phys. Rev. (Ser. 2), vol. 73, 1948, pp. 526-527.
27. Beck, P. A., Towers, J., Jr., and Manley, W. D.: Grain Growth in 70-30 Brass. Trans. AIME, vol. 175, 1948, pp. 162-177.
28. Burke, J. E.: Grain Growth in Alpha-Brass. Jour. Appl. Phys., vol. 18, no. 11, Nov. 1947, p. 1028.
29. Larson, F. R., and Salmas, J.: A Time-Temperature Relationship for Recrystallization and Grain Growth. Trans. ASM, vol. 46, 1954, pp. 1377-1405.
30. Underwood, E. E., Wolff, A. K., Marsh, L. L., and Manning, G. K.: The Principles of Dispersion Hardening Which Promote High-Temperature Strength in Iron-Base Alloys. WADC TR 56-184, Pt. III, Contract AF-33(616)-2785, WADC and Battelle Mem. Inst., Apr. 1958.
31. Hillert, M.: Pressure-Induced Diffusion and Deformation During Precipitation, Especially Graphitization. Jernkontorets Ann., vol. 141, 1957, pp. 67-89.

TABLE I.- SPECTROGRAPHIC AND CHEMICAL ANALYSIS  
OF ALUMINUM-COPPER ALLOYS

Nominal composition, weight percent copper	Chemical analysis, weight percent copper	Spectrographic analysis, ppm			
		Si (a)	Fe	Pb	Mg
1	0.99 1.04 1.05 1.04	20	20	b <sub>nd</sub>	1.0
2	2.04 2.07 2.07 2.04	20	b <sub>nd</sub>	b <sub>nd</sub>	1.0
3	3.05 3.08 2.95 3.14	20	b <sub>nd</sub>	b <sub>nd</sub>	1.0
4	4.03 4.07 4.14 4.11	20	b <sub>nd</sub>	20	1.0

<sup>a</sup> Si pickup possible from the electrode.

<sup>b</sup> nd = not detected (<20 ppm).

TABLE II.- HEAT TREATMENT AND PROCEDURES FOR  
OBTAINING INITIAL GRAIN SIZES

Nominal composition, weight percent copper	Final cold reduction, percent	Specimen thickness, in.	Min	Temperature, °C	Grain size (a)	
					ASTM	mm
1	50	0.125	1/2	540	1	0.213
2	40	.125	1	540	1	.213
3	20	.125	200	540	-3	.833
	20	.125	3	540	1	.213
	42.5	.090	1/2	470	3	.105
4	10	.125	6	540	1	.213

<sup>a</sup>Average grain diameter calculated from number of grain-boundary intercepts per unit length of random traverses across microstructure.

TABLE III.- CREEP DATA FOR ALLOY OF 3 PERCENT COPPER  
OVERAGED AT 390° C

Time, min	Strain, percent	Total volume of precipitate, percent	300° C and 2,400 psi			
			Volume of fine particles, percent	Volume of large particles, percent	Grain diameter, mm	Particle radius, mm
0	----	1.95	----	----	0.0319	-----
5	0.85	2.28	1.93	0.35	.0316	0.0178
10	1.38	2.86	1.61	1.25	.0276	.0207
20	3.48	2.16	1.88	.28	.0357	.0169
33	4.70	1.47	1.11	.36	.0455	.0278
45	9.98	2.85	1.57	1.28	.0394	.0214

TABLE IV.- TENSILE DATA

$$[\dot{\epsilon} = 0.0314 \text{ min}^{-1}]$$

Composition, percent Cu	Solution time, min	Strain at maximum load, percent	Ultimate tensile strength, psi	Matrix composition, percent Cu	Tensile strength of matrix, psi	Tensile strength, psi	Spacing, mm
2	0	32.2	16,950-17,350	1.1	17,000	350	0.025
	10	27.3	26,250-26,450	.25	10,300	16,150	.0724
	35	28.2	26,400-26,450	1.2	18,200	8,250	.109
	60	27.0	28,500	1.5	22,200	6,300	.181
	120	28.4	26,300	2.2	30,100	-3,800	.194
3	0	27.1	26,000-26,150	1.3	19,500	6,650	0.035
	1/2	25.6	27,150	1.1	17,000	10,150	(~.055)
	3	29.7	34,000	1.8	26,300	7,700	.117
	10	28.2	35,000	2.5	31,900	3,100	.215
	40	26.1	35,500	2.3	30,700	4,800	.369
4	0	27.1	31,800	1.9	27,500	4,300	0.014
	1/2	31.5	31,800	2.1	29,500	2,300	-----
	1	27.9	32,100	1.9	27,500	4,600	-----
	2-1/2	33.2	34,650	2.3	30,700	3,950	-----
	5	24.2	36,100	2.6	32,400	3,700	.533

TABLE V.- LATTICE PARAMETERS OF ALUMINUM-COPPER ALLOYS  
AS A FUNCTION OF DISSOLUTION TIME

Dissolution temperature, °C	Time, min	Lattice parameter, A.U.	Copper content, weight percent
2 percent copper			
430	0	$4.0470 \pm 0.0007$	1.1
	10	$4.0489 \pm .0005$	.25
	35	$4.0467 \pm .0006$	1.2
	60	$4.0459 \pm .0007$	1.5
	120	$4.0445 \pm .001$	2.2
3 percent copper			
470	0	$4.0464 \pm 0.001$	1.3
	1/2	$4.0468 \pm .0008$	1.1
	3	$4.0453 \pm .0006$	1.8
	10	$4.0437 \pm .0006$	2.5
	40	$4.0442 \pm .001$	2.3
4 percent copper			
510	0	$4.0451 \pm 0.0005$	1.9
	1/2	$4.0446 \pm .0005$	2.1
	1	$4.0451 \pm .0005$	1.9
	2-1/2	$4.0442 \pm .0008$	2.3
	5	$4.0435 \pm .0007$	2.6

TABLE VI.- GRAIN DIAMETERS WITHOUT STRESS AND SLOPES n FOR ASTM +1

(a) 1 percent copper

420° C		460° C		500° C		540° C		580° C	
Time, min	Diameter, mm	Time, min	Diameter, mm	Time, min	Diameter, mm	Time, min	Diameter, mm	Time, min	Diameter, mm
0	0.234	0	0.244	0	0.224	0	0.216	0	0.216
16	.249	20	.471	20	.730	15	.767	10	.829
70	.298	60	.497	65	.760	30	.719	20	1.144
95	.346	90	.492	110	.938	60	1.087	30	1.220
200	.345	130	.685	145	.698	90	1.113	50	1.480
360	.316	220	.781	240	1.00	120	1.012	75	1.513
415	.357	400	.786			185	1.227	100	1.350
						.5	.290		
						1.1	.211		
						2.0	.340		
						3.0	.402		
						4.0	.467		
						5.0	.412		
						0	.320		
						.4	.224		
						5	.373		
						10	.568		
						20	.700		
						60	1.16		
						100	1.60		
n = 0.042		n = 0.155		n = 0.214		n = 0.282		n = 0.359	

TABLE VI.- GRAIN DIAMETERS WITHOUT STRESS

AND SLOPES  $n$  FOR ASTM +1 - Continued

(b) 2 percent copper

460° C		500° C		540° C		580° C	
Time, min	Diameter, mm	Time, min	Diameter, mm	Time, min	Diameter, mm	Time, min	Diameter, mm
0	0.191	0	0.159	0	0.154	0	0.145
20	.243	10	.344	15	.504	10	.649
60	.368	20	.441	30	.689	20	.850
90	.435	40	.474	60	.688	30	.825
130	.405	64	.564	90	.930	50	1.21
220	.480	106	.540	120	.822	75	1.25
400	.464	215	.862	165	.867	100	1.43
				0	.279		
				.6	.179		
				7	.382		
				18	.475		
				40	.529		
				75	.595		
				110	.992		
				3	.348		
				3.7	.379		
				5	.370		
				7	.433		
				10	.497		
$n = 0.180$		$n = 0.233$		$n = 0.291$		$n = 0.380$	

TABLE VI.- GRAIN DIAMETERS WITHOUT STRESS  
AND SLOPES  $n$  FOR ASTM +1 - Continued

(c) 3 percent copper

460° C		500° C		540° C		570° C	
Time, min	Diameter, mm	Time, min	Diameter, mm	Time, min	Diameter, mm	Time, min	Diameter, mm
0	0.202	0	0.273	0	0.208	0	0.258
15	.226	10	.390	8	.283	10	.826
40	.189	25	.532	20	.417	20	.705
80	.182	50	.619	45	.521	40	.900
140	.210	102	1.01	85	.741	60	1.53
245	.212	140	1.07	120	.736	90	1.36
460		214					
			1.011		.167		
				2.5			
				4	.296		
				6	.274		
				10	.334		
				15	.390		
				8	.283		
				20	.417		
				45	.521		
				85	.741		
				120	.736		
				480	1.40		
				990	1.77		
				1,200	1.75		
				1,440	2.46		
				2,880	3.30		
$n = 0.071$		$n = 0.316-0.355$		$n = 0.394$		$n = 0.423-0.502$	

TABLE VI.- GRAIN DIAMETERS WITHOUT STRESS

AND SLOPES  $n$  FOR ASTM +1 - Concluded

(d) 4 percent copper

520° C		540° C		560° C	
Time, min	Diameter, mm	Time, min	Diameter, mm	Time, min	Diameter, mm
0	0.219	0	0.094	0	0.205
15	.217	10	.200	10	.325
30	.315	22	.382	20	.390
60	.442	60	.650	40	.668
90	.595	105	.621	60	.660
130	.595	150	.863	100	.906
180				140	
	.624		.23		.752
		7	.26		
		10			
		14	.268		
		20	.386		
		5.33	.20		
		10	.20		
		22	.38		
		60	.65		
		105	.62		
		150	.86		
$n = 0.419$		$n = 0.442$		$n = 0.457-0.501$	

TABLE VII.- GRAIN DIAMETERS WITHOUT STRESS  
AND SLOPES  $n$  FOR ASTM +3 AND ASTM -3

500° C		540° C		570° C	
Time, min	Diameter, mm	Time, min	Diameter, mm	Time, min	Diameter, mm
3 percent copper (ASTM +3)					
0	0.270	0	0.224	0	0.292
2	.458	4	.733	1	.455
5	.538	8	1.06	3	.700
10	.666	15	.848	7	.970
20	.910	30	1.245	15	.961
40	.803	60	1.267	30	1.29
80	.893	100	1.27	60	2.35
120	1.228	200	1.68	100	1.48
200				200	
	1.34	0	.320		5.55
		10	.847		
		20	1.230		
		45	1.345		
		85	1.882		
		100	1.515		
n = 0.175		n = 0.204		n = 0.212	
3 percent copper (ASTM -3)					
0	1.52	0	1.58	0	1.31
10	1.36	10	1.30	10	1.50
20	1.71	20	1.44	20	1.26
40	1.58	40	1.53	40	1.51
80	1.53	80	1.18	70	1.39
180	1.73	130	2.19	120	1.59
300	1.51	200	1.57	180	1.65
n = 0.0		n = 0.046		n = 0.0624	

TABLE VIII.- GRAIN DIAMETERS WITH STRESS

AND SLOPES  $n$  FOR ASTM +1

(a) 1 percent copper

540° C; 85 psi			540° C; 200 psi		
Time, min	Diameter, mm	Strain, percent	Time, min	Diameter, mm	Strain, percent
0	~0.14	-----	0	~0.14	-----
25	.473	1.43	10	.272	1.48
50	1.10	1.60	20	.598	1.85
173	1.52	1.96	40	.925	4.95
678	1.92	4.52	60	1.19	5.65
1,107	3.57	9.70	152	1.616	32.2
			193		
				1.195	33.6
$n = 0.459$			$n = 0.552$		

(b) 2 percent copper

540° C; 85 psi			540° C; 140 psi			540° C; 200 psi		
Time, min	Diameter, mm	Strain, percent	Time, min	Diameter, mm	Strain, percent	Time, min	Diameter, mm	Strain, percent
0	~0.26	-----	0	~0.24	-----	0	~0.24	-----
21	.347	1.44	25	.419	1.5	25	.667	1.8
50	.694	1.62	50	1.10	1.9	50	1.088	3.5
98	1.10	1.7	105	.915	3.0	100	1.125	7.1
200	1.34	1.8	171	1.22	4.0	175	1.076	12.3
505	1.47	3.0	402	1.82	9.0	367	2.10	37.3
1,320	2.68	6.5	1,413	2.60	35.3			
$n = 0.344$			$n = 0.371$			$n = 0.387$		

TABLE VIII.- GRAIN DIAMETERS WITH STRESS  
AND SLOPES  $n$  FOR ASTM +1 - Concluded

(c) 3 percent copper

540° C; 200 psi			540° C; 200 psi			570° C; 200 psi		
Time, min	Diameter, mm	Strain, percent	Time, min	Diameter, mm	Strain, percent	Time, min	Diameter, mm	Strain, percent
0	~0.27	----	0	~0.28	----	0	~0.28	----
25	.292	1.4	22	.357	1.8	16	.435	2.1
56	.430	1.8	40	.635	2.4	30	.699	3.1
100	.564	2.3	80	.781	4.0	50	.970	5.9
335	.820	6.0	190	1.241	10.2	95	1.26	12.7
1,440	1.392	25.9	423	1.625	22.0	166	1.42	24.0
$n = 0.385$			$n = 0.418-0.495$			$n = 0.442-0.519$		

(d) 4 percent copper

540° C; 200 psi		
Time, min	Diameter, mm	Strain, percent
0	~0.20	----
25	.240	1.8
50	.400	2.7
100	.719	4.5
185	.788	6.8
433	1.122	21.2
$n = 0.511$		

TABLE IX.- GRAIN DIAMETERS WITH STRESS AND  
SLOPES  $n$  FOR ASTM +3 AND ASTM -3

500° C; 200 psi			540° C; 200 psi			570° C; 200 psi		
Time, min	Diameter, mm	Strain, percent	Time, min	Diameter, mm	Strain, percent	Time, min	Diameter, mm	Strain, percent
3 percent copper (ASTM +3)								
0	~0.12	-----	0	~0.13	-----	0	~0.14	-----
20	.526	1.36	20	.768	1.73	24	.962	2.13
50	.838	1.39	40	1.18	3.22	40	1.20	5.42
92	1.055	2.17	83	1.47	5.39	70	1.44	9.50
156	1.224	3.68	204	1.58	13.92	120	1.65	18.97
305	1.125	6.71	536	2.25	45.84	185	1.80	28.47
1,285	1.890	22.55						
n = 0.226			n = 0.250			n = 0.264		
3 percent copper (ASTM -3)								
0	~1.5	-----	0	~1.4	-----	0	~1.5	-----
50	1.62	1.68	34	2.09	2.19	30	1.52	3.53
100	1.53	2.29	62	1.51	3.63	60	1.98	7.79
150	1.57	3.14	112	2.10	6.46	100	2.23	11.94
411	2.25	8.15	220	2.25	9.89	148	2.15	19.01
1,381	2.49	21.13	466	3.41	18.55	235	2.40	32.37
n = 0.129			n = 0.143			n = 0.147		

TABLE X.- PARTICLE DISSOLUTION DATA WITHOUT STRESS

Temperature, °C	Time, min	Volume of precipitate, percent	Spacings, mm	Grain size, mm
2 percent copper overaged at 351° C				
415	0	1.38	0.025	0.137
	2	1.18	.0281	.0168
	5	.780	.0352	.0172
	10	.889	.0724	.0352
	20	.830	.0925	.0529
	35	.563	.109	.0758
	60	.279	.181	.128
	120	.392	.194	.129
3 percent copper overaged at 390° C				
470	3	-----	0.117	-----
	10	-----	.215	-----
	15	-----	.181	-----
	25	-----	.335	-----
	40	-----	.369	-----
	60	-----	(.240)	-----
	120	-----	.587	-----
500	0	1.95	0.035	0.0308
	1	.89	.206	.127
	3	.78	.265	.189
	5	.576	.335	.202
	10	.236	.840	.278
	15	.297	.840	.323
	25	.252	.952	.408
	40	.282	1.42	.467
	55	.114	2.95	.725
	70	.102	3.54	.680
	90	.045	11.5	.543
	120	.015	49.5	.715
540	1	(0.065)	(8.47)	-----
	3	.0953	7.10	-----
	5	.083	8.13	-----
570	1	0.174	2.67	-----
	2	.052	7.30	-----
	4	.0093	77.0	-----
4 percent copper overaged at 420° C				
510	0	3.77	0.0142	-----
	5	1.13	.533	0.70
	12	.55	.691	.48
	20	.310	1.28	.59
	35	.395	1.36	.58
	60	.230	2.48	1.00
	120	.045	4.44	1.11

TABLE XI.- PARTICLE DISSOLUTION DATA WITH STRESS

Temperature, °C	Stress, psi	Time, min	Volume of precipitate, percent	Particle spacing, mm	Strain, percent
3 percent copper overaged at 390° C					
500	200	15	0.264	1.57	1.53
		30	.170	2.15	1.59
		45	.084	4.23	1.67
		60	.128	3.37	1.86
		80	.051	7.86	1.94
		100	.100	4.63	2.36
	500	8	0.295	0.329	2.0
		20	.243	.685	5.0
		34	.128	1.34	8.8
		46	.112	1.81	10.7
		60	.100	3.20	21.7
	800	3	2.21	-----	1.2
		6	1.37	-----	1.8
		10	.216	0.262	5.5
		14	.177	.883	13.2
		18.3	.214	.929	27.0
	200	10	0.0736	4.18	1.7
		20	.1270	5.17	1.9
		30	.0236	24.8	2.8
		40	.0	-----	2.9
540	200	5	0.275	1.35	1.5
		10	(.0014)	80.0	2.1
		15	.0	-----	2.7

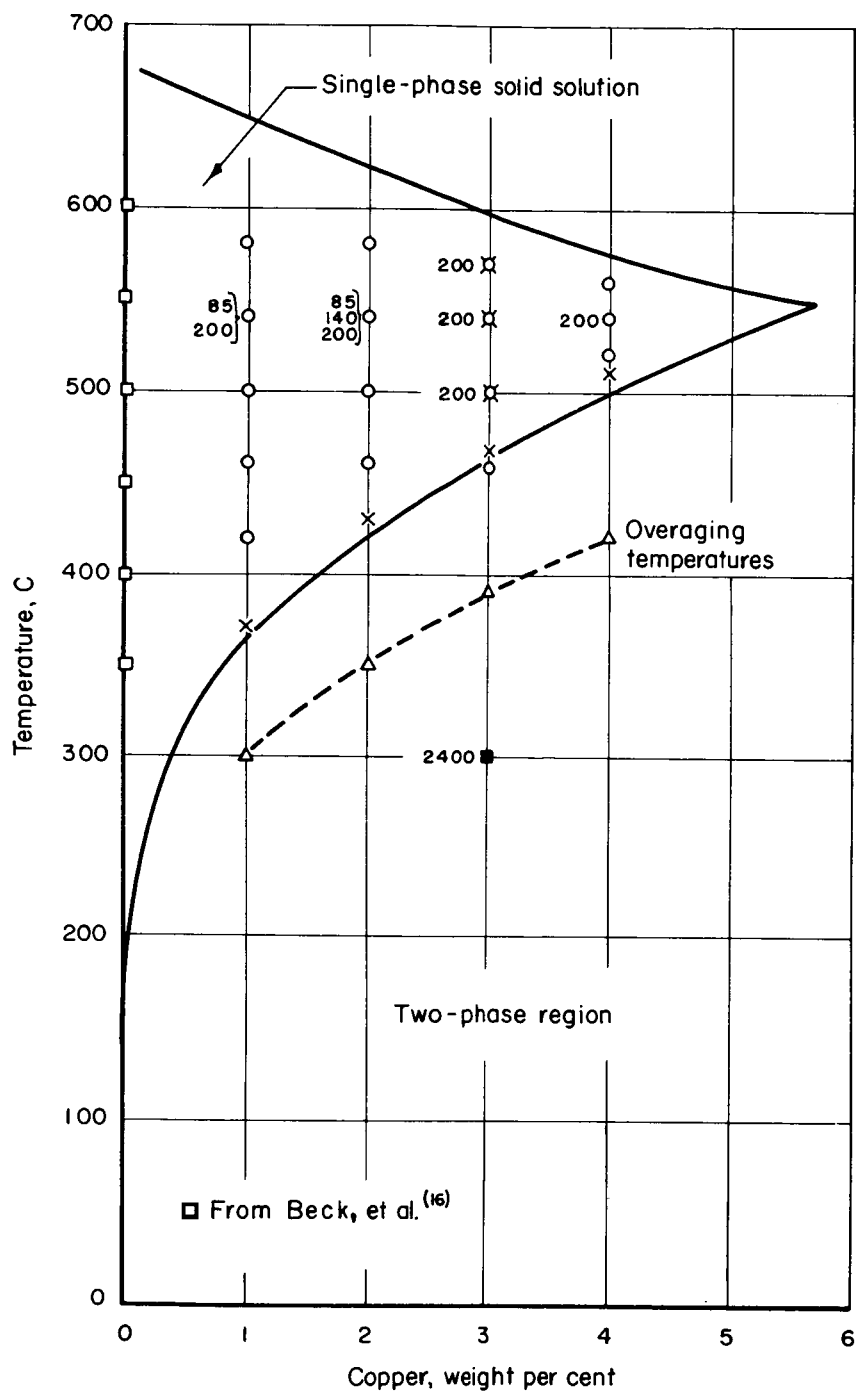


Figure 1.- Aluminum-copper phase diagram showing compositions tested and heat treated. Numbers to left of symbols represent stresses used in psi.

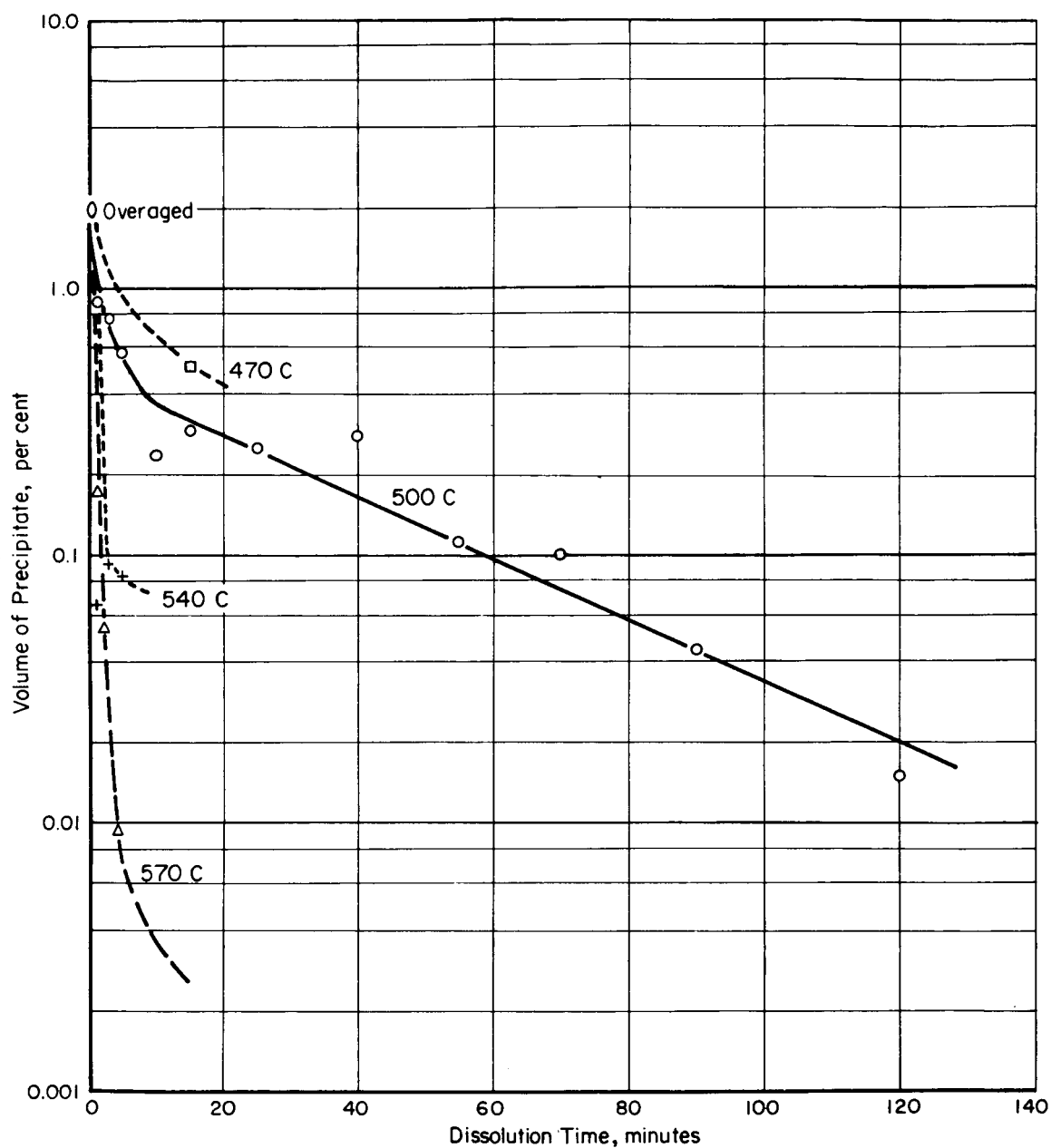


Figure 2.- Dissolution of precipitate particles in Al-3Cu alloys in single-phase region, without stress.

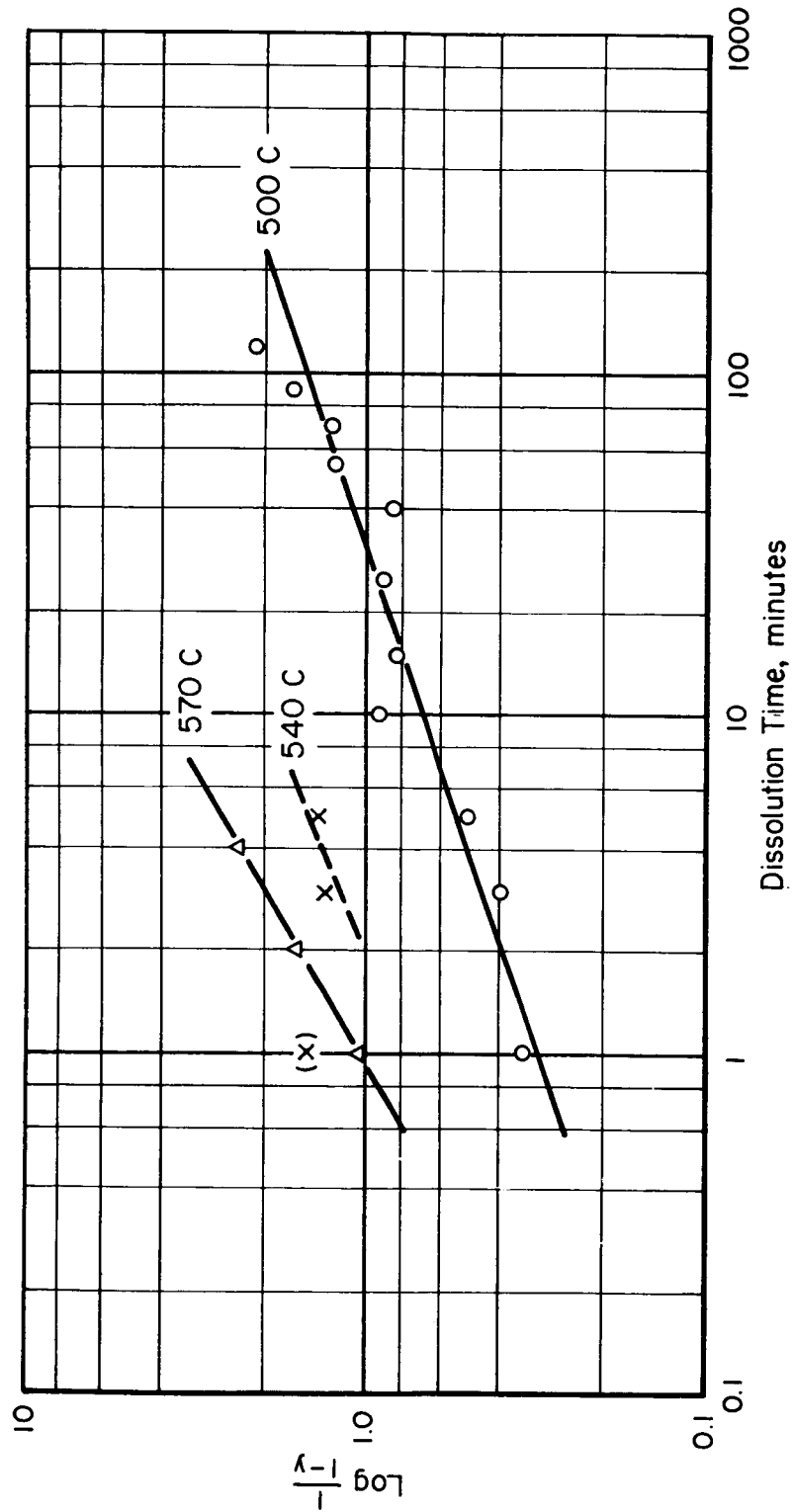


Figure 3.- Dissolution of particles in overaged Al-3Cu alloys, without stress, according to kinetic analysis.

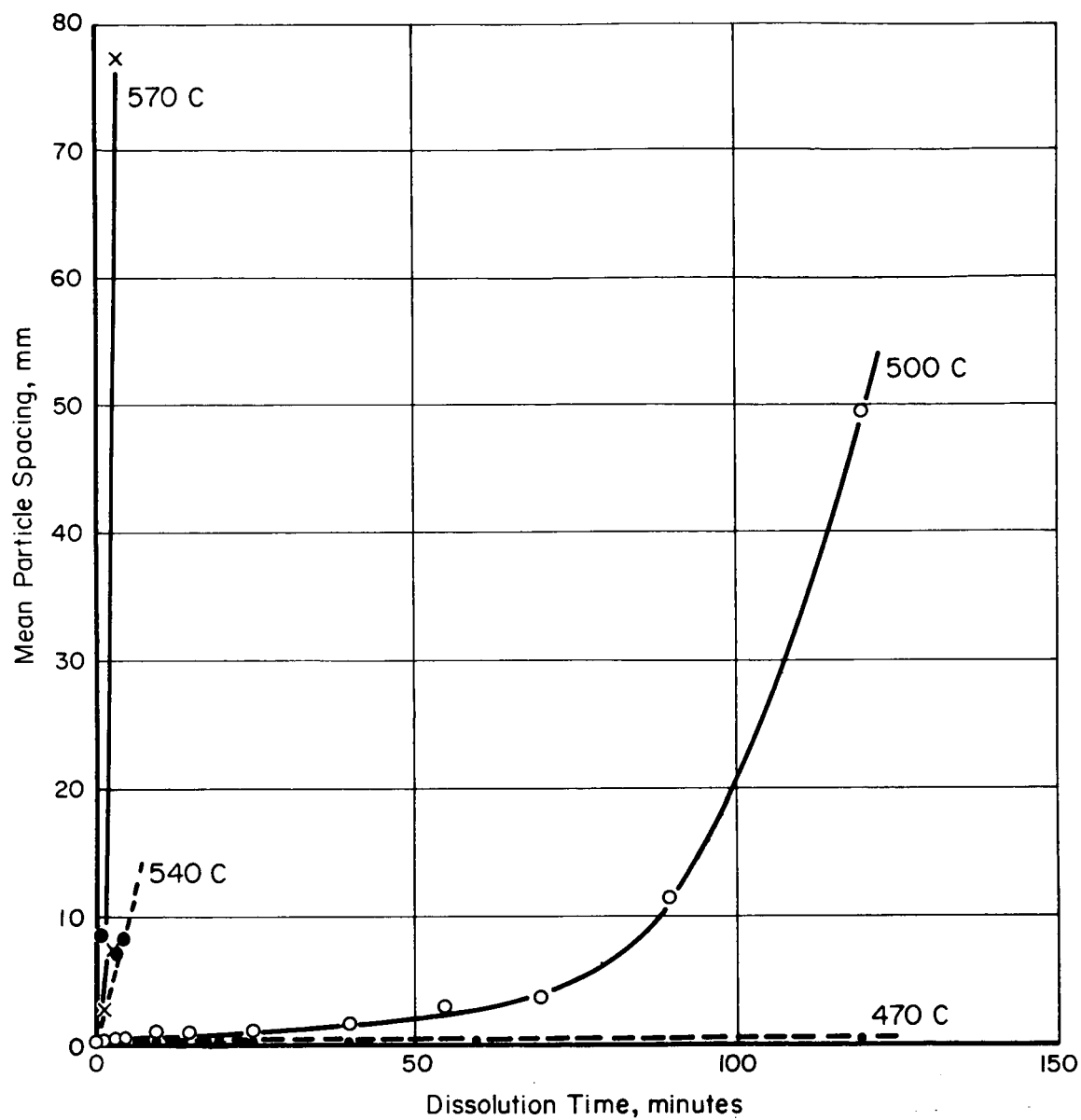


Figure 4.- Change in particle spacing as a function of dissolution time for Al-3Cu alloys at various single-phase temperatures, without stress.

W-119

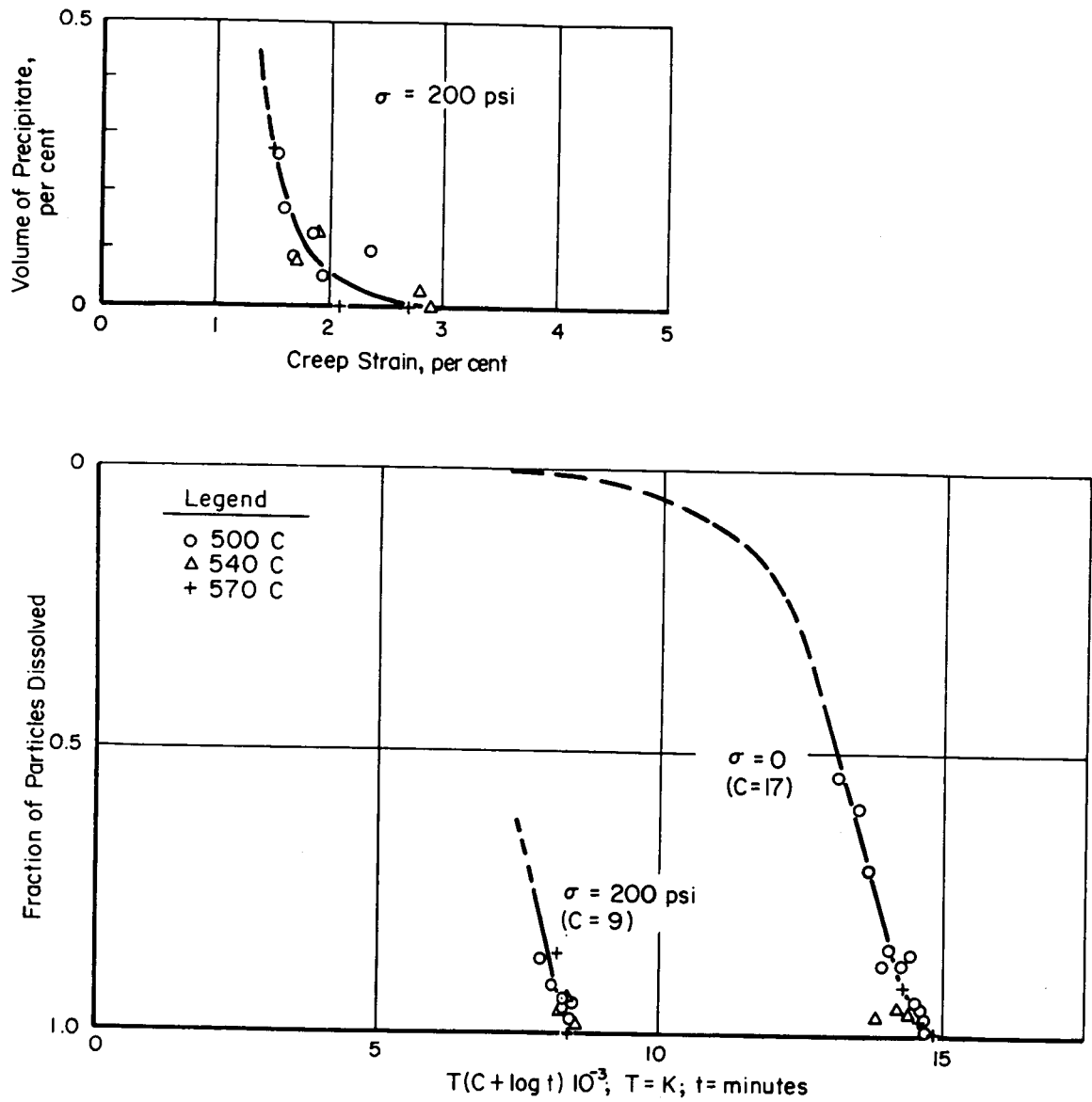


Figure 5.- Particle dissolution as a function of creep strain and of a time-temperature parameter, in overaged Al-3Cu alloys.

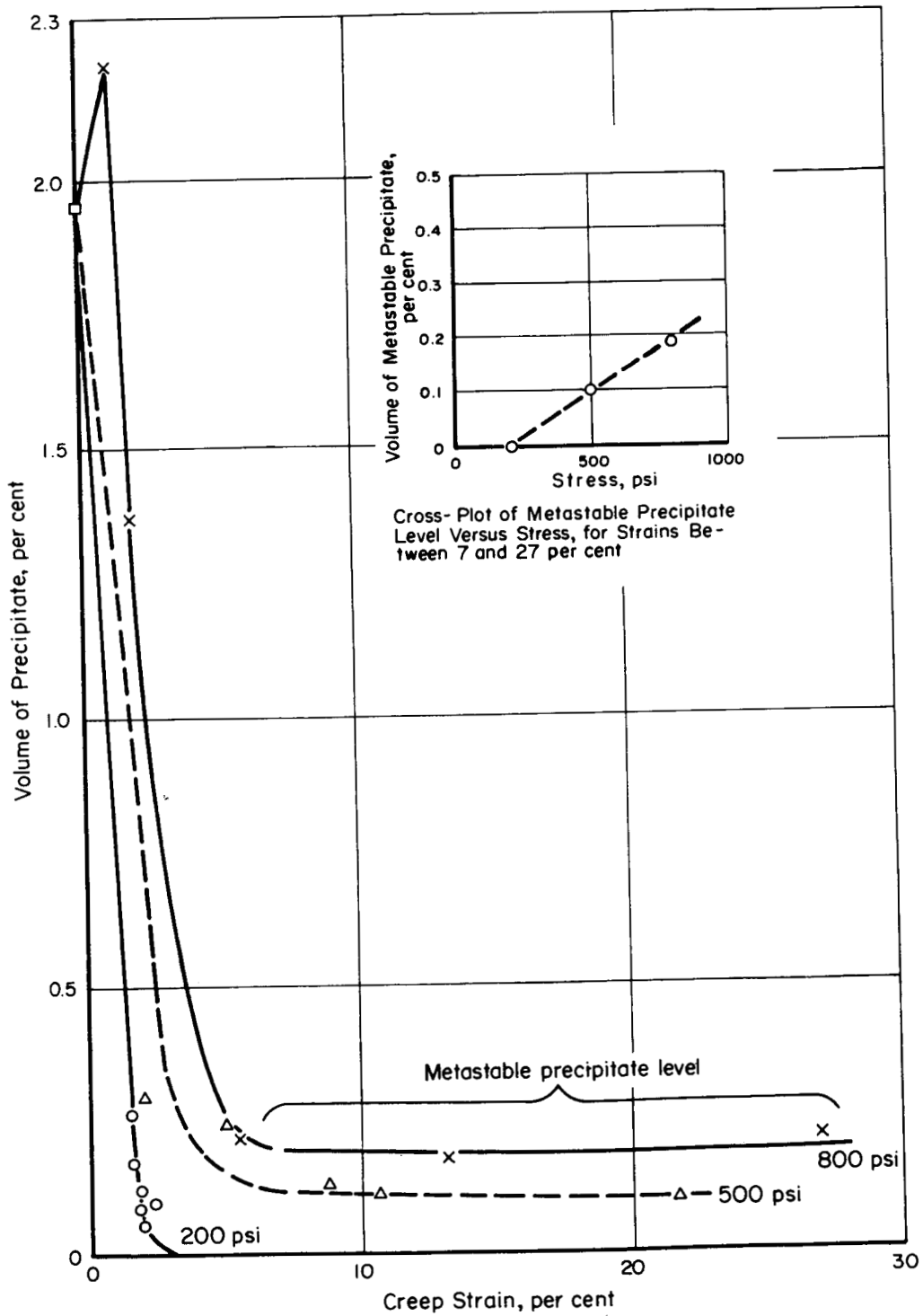


Figure 6.- Particle dissolution as a function of creep strain in over-aged Al-3Cu alloys at 500° C.

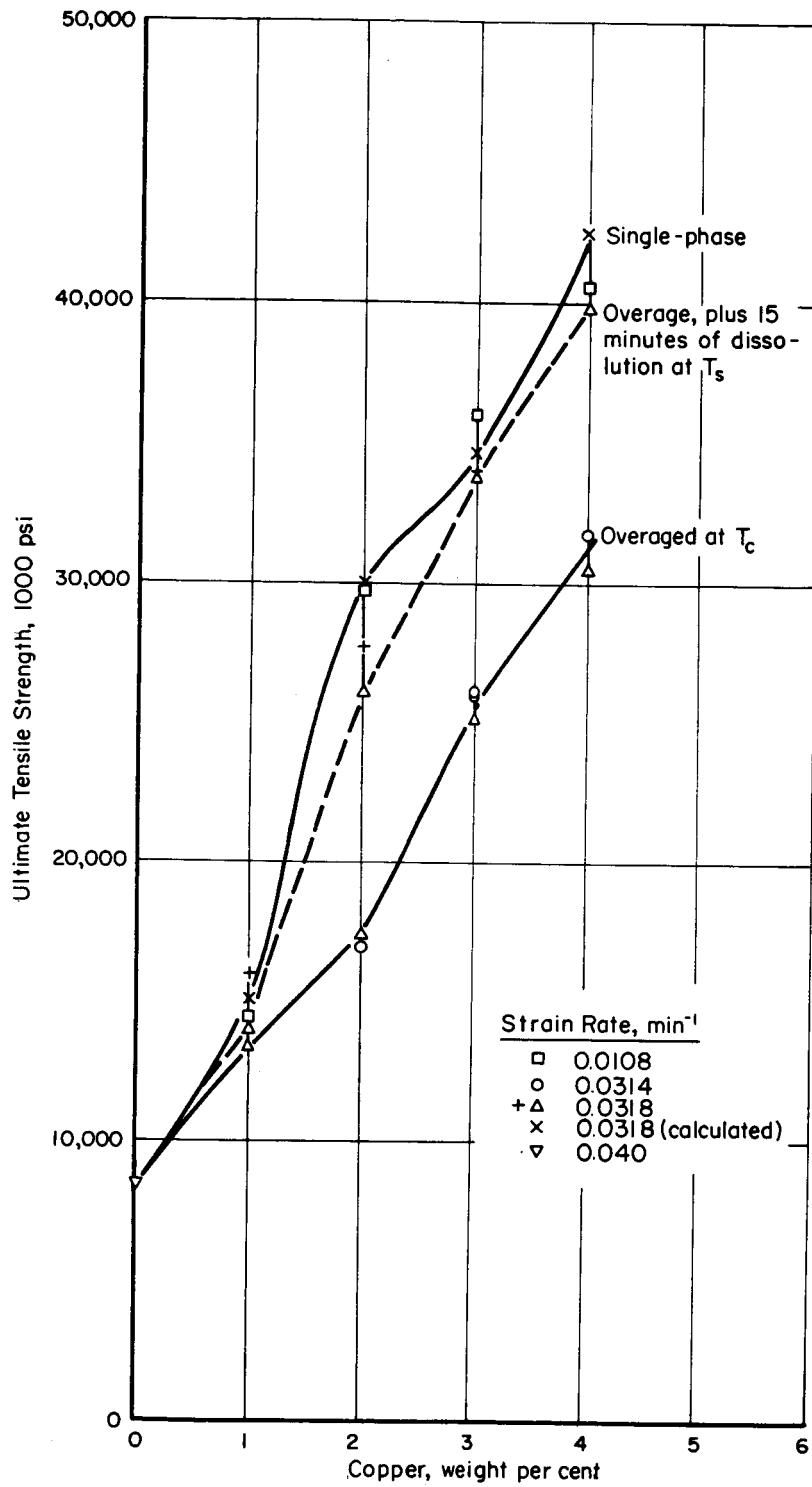


Figure 7.- Room-temperature tensile strength of aluminum-copper alloys.

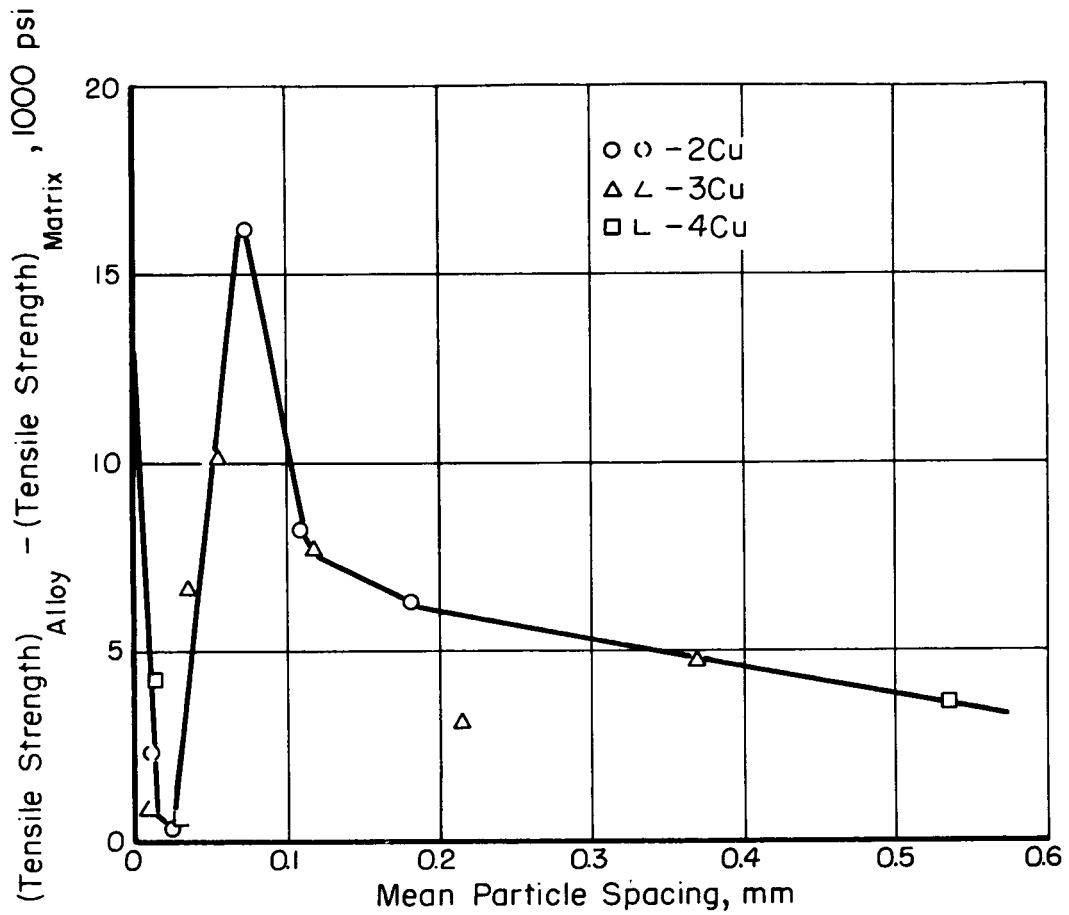


Figure 8.- Particle-strengthening increment in particulate aluminum-copper alloys at room temperature.

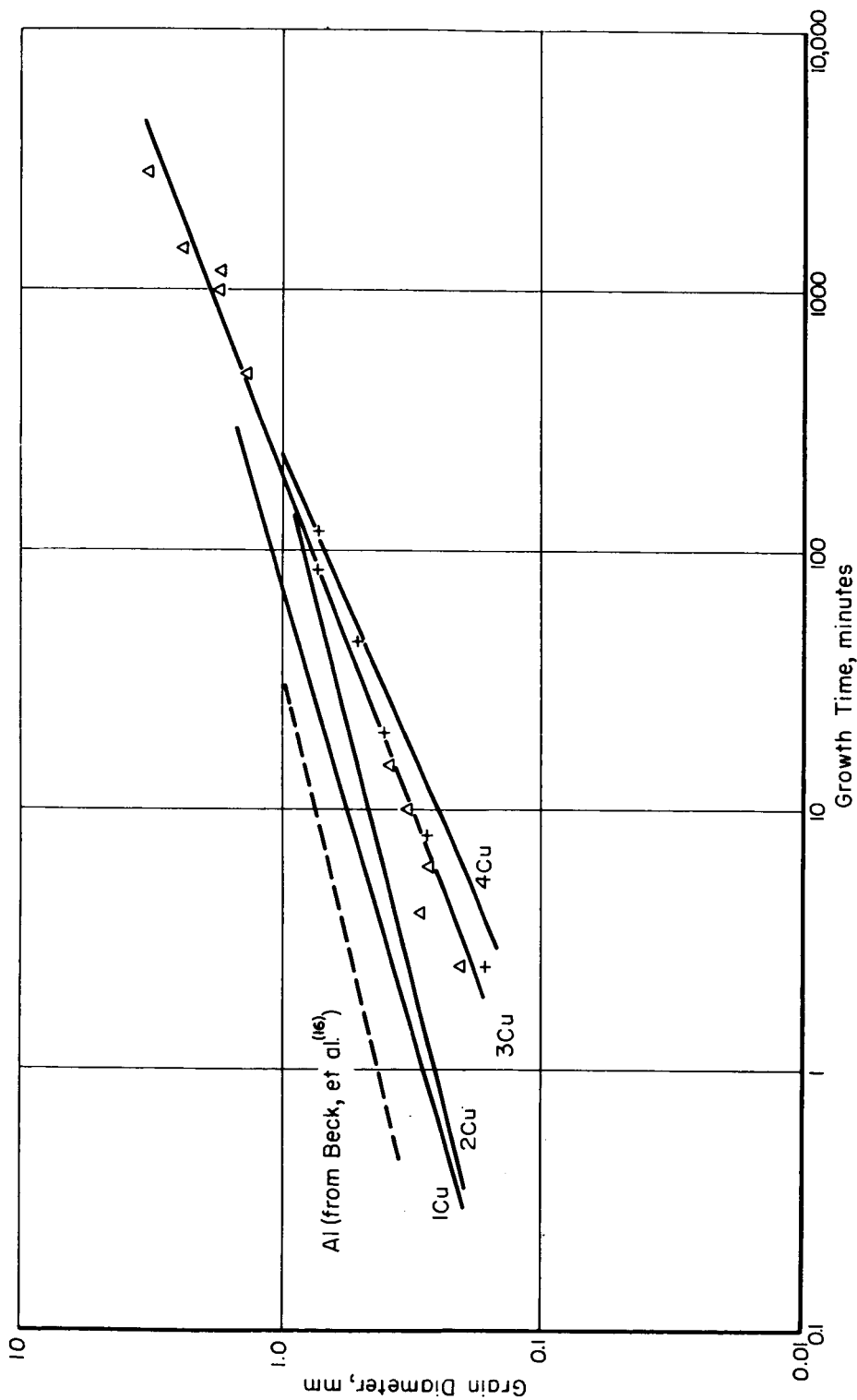


Figure 9.- Grain growth in aluminum-copper alloys at 540° C without applied stress. Initial grain size: ASTM 1.

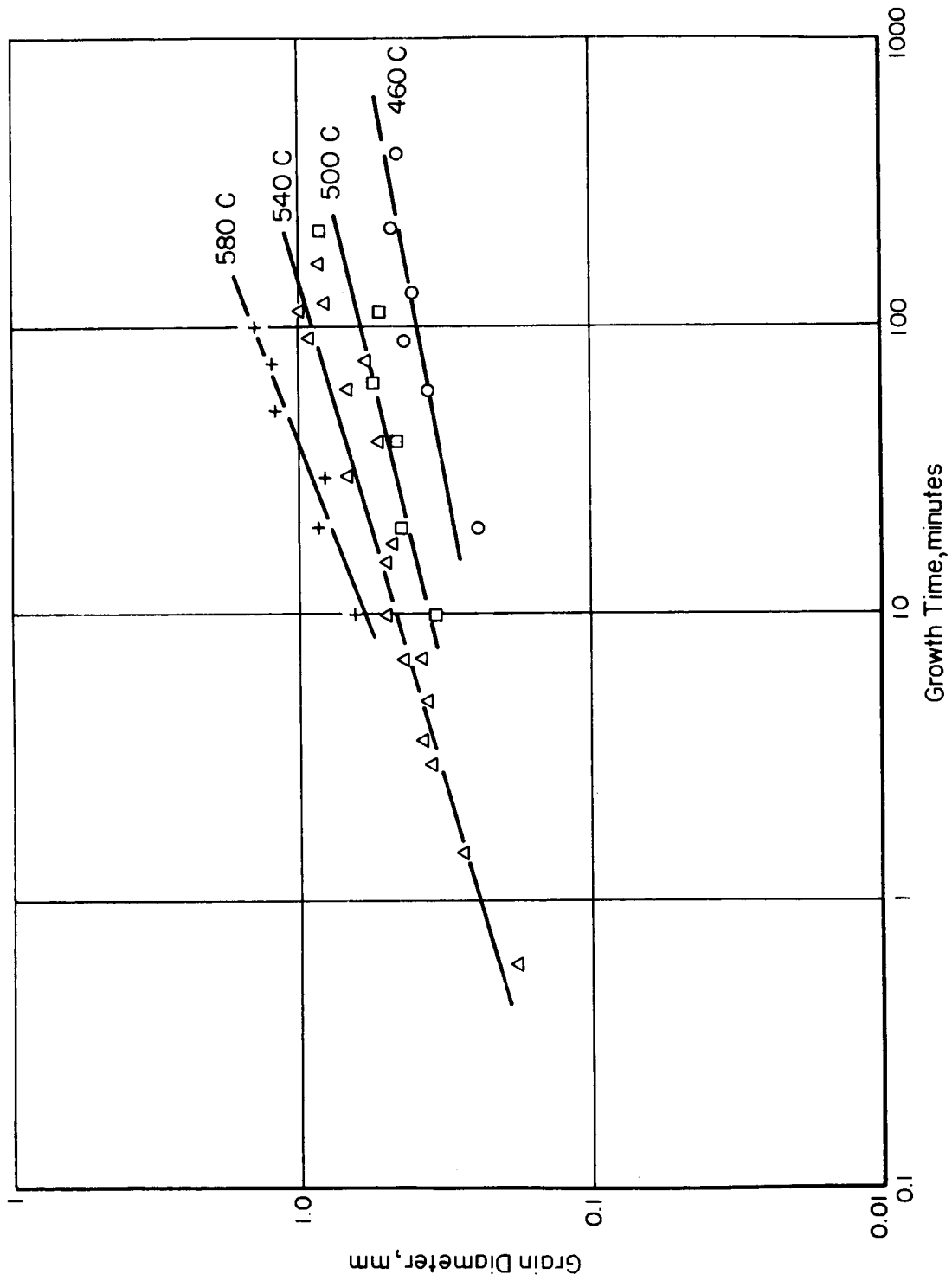


Figure 10.- Grain growth in Al-2Cu alloys without applied stress. Initial grain size: ASTM 1.

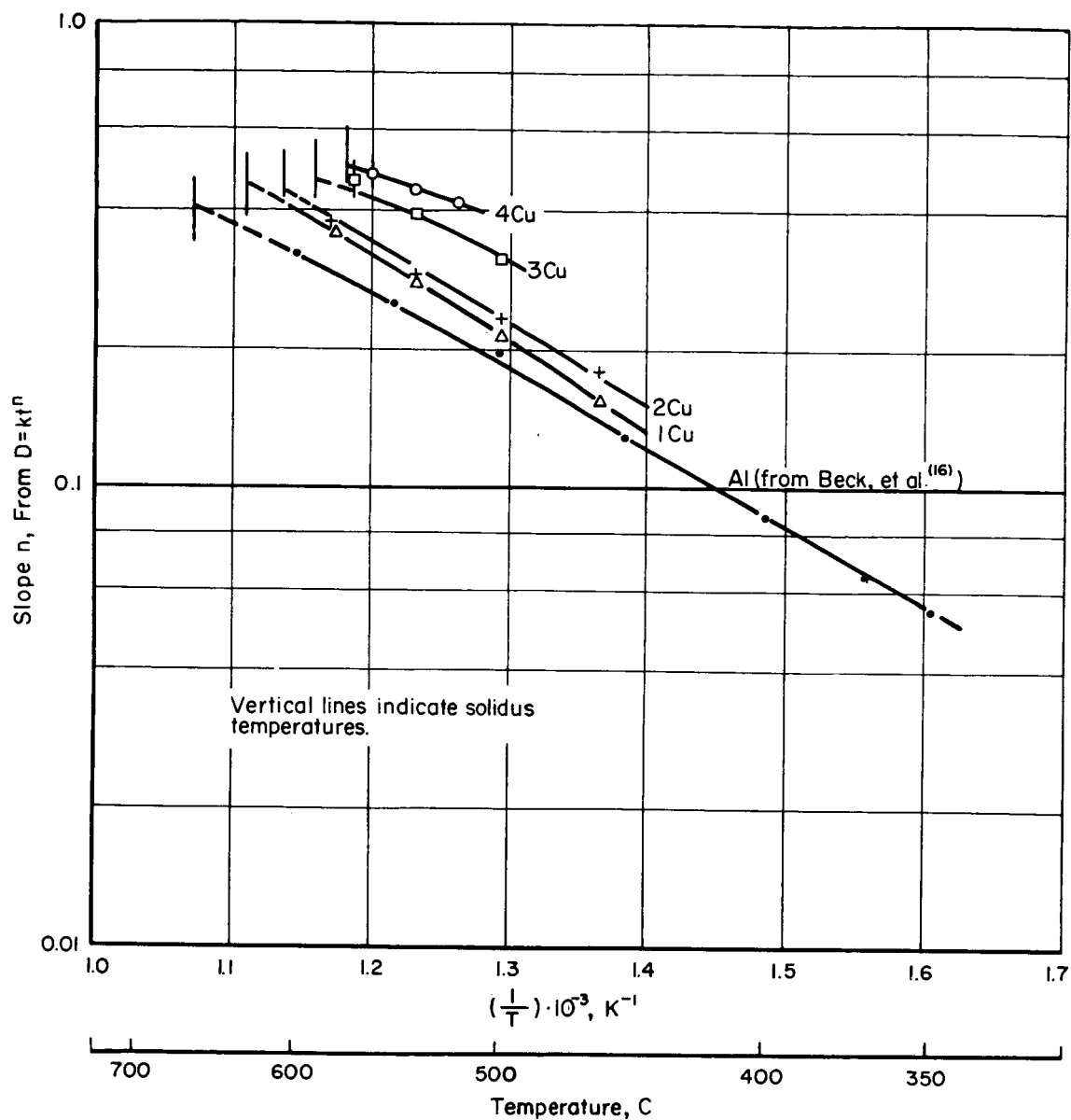


Figure 11.- Slope of curves of grain growth without applied stress as a function of reciprocal temperature for aluminum-copper alloys. Initial grain size: ASTM 1.

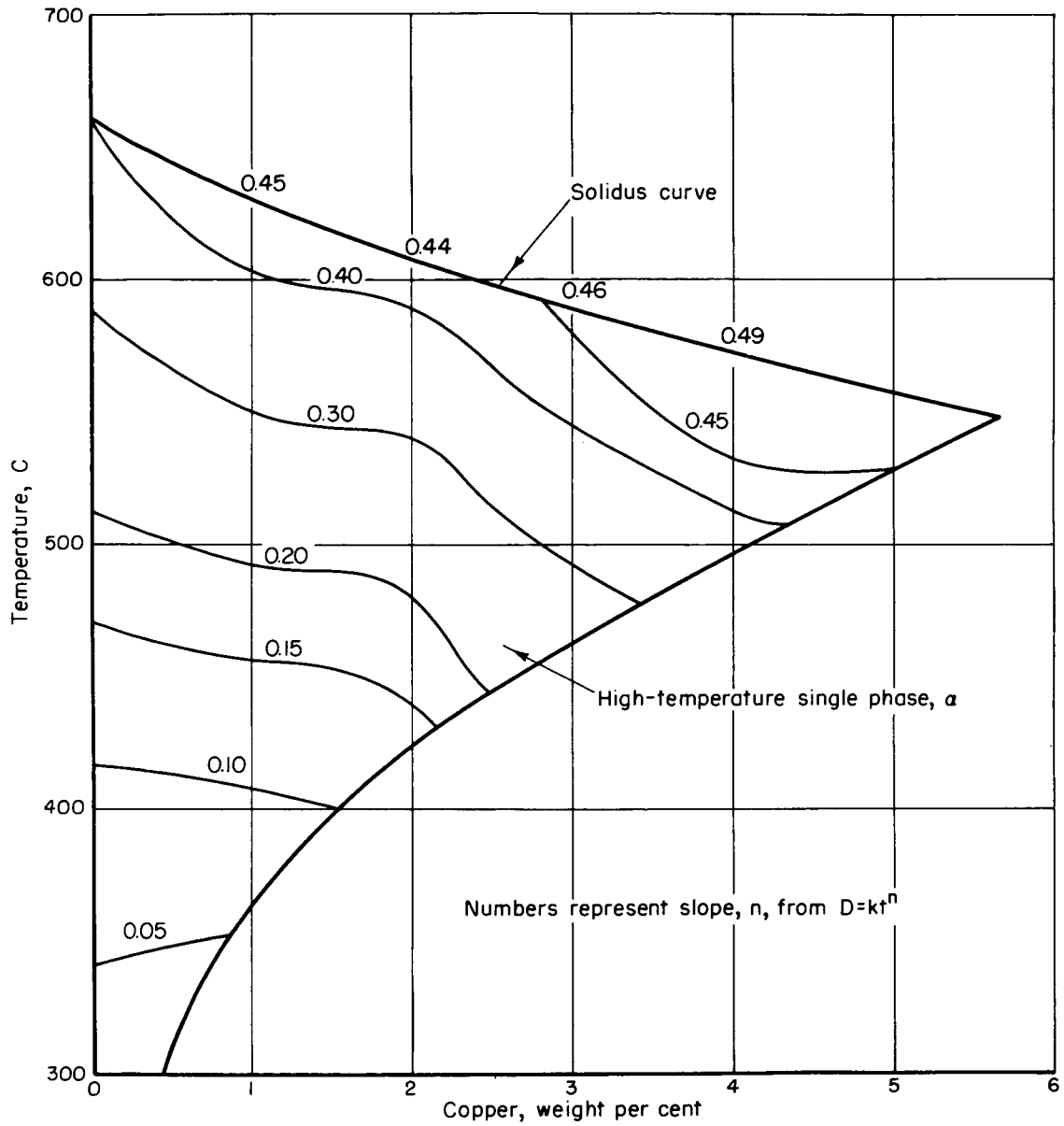


Figure 12.- Slopes of grain-growth curves of equal value superimposed on aluminum-rich portion of aluminum-copper phase diagram. Initial grain size: ASTM 1.

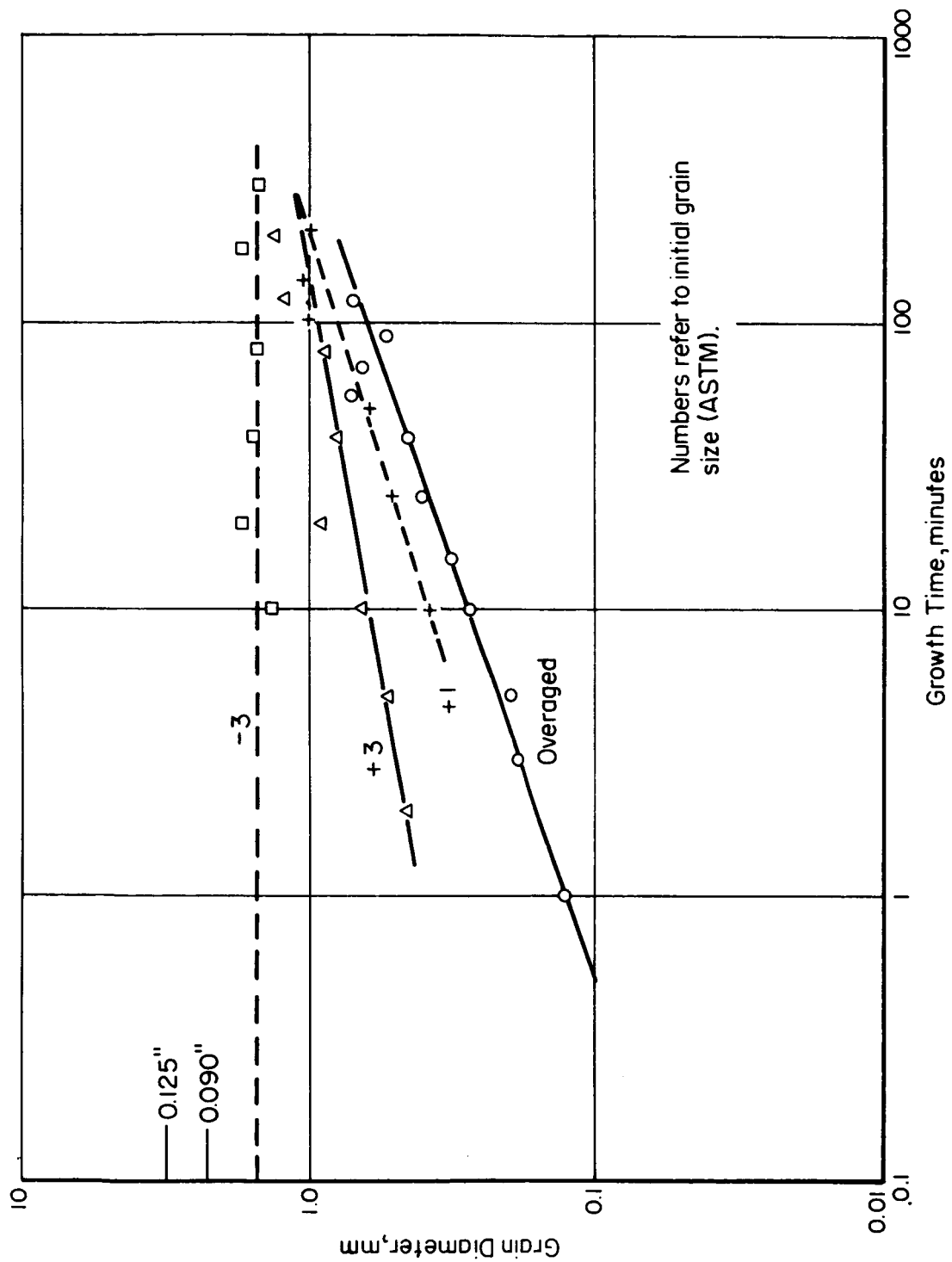


Figure 13.- Grain growth in single-phase or overaged Al-3Cu alloys at 500° C without stress.

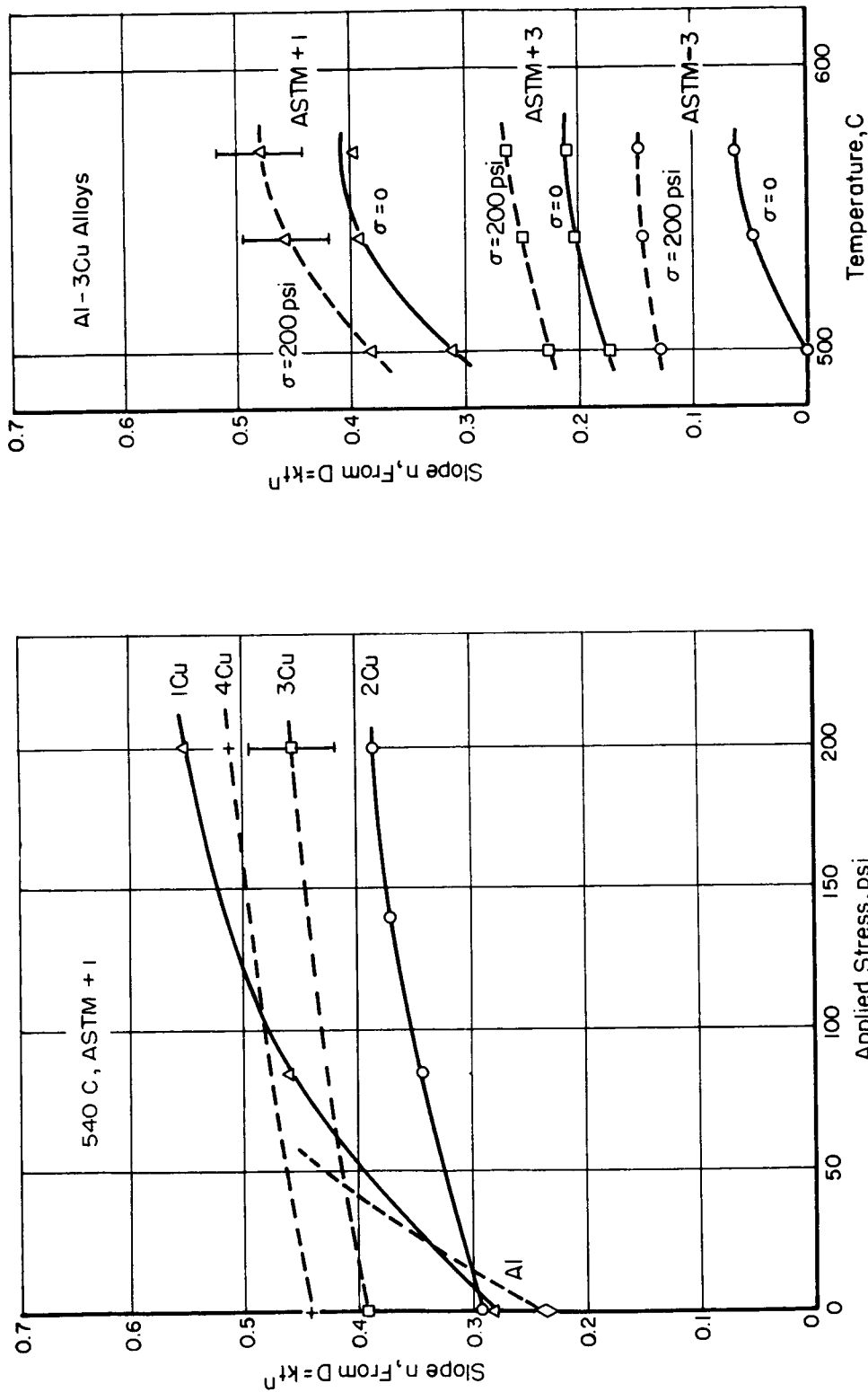


Figure 14.- The stress and temperature dependence of the slope of grain-growth curves for aluminum-copper alloys as a function of initial grain size.

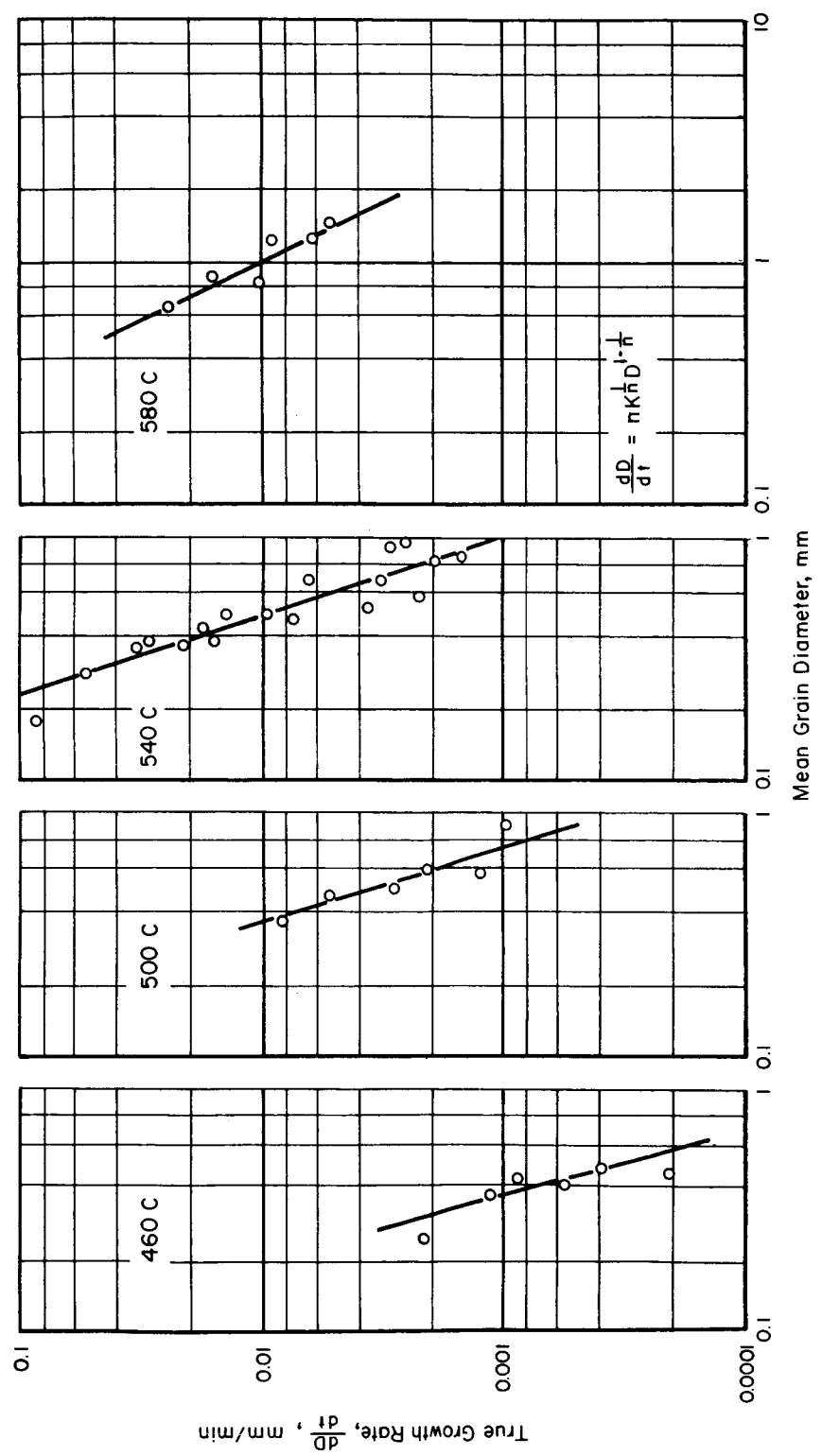


Figure 15.- True growth rate as a function of grain diameter for Al-2Cu alloys, without applied stress.

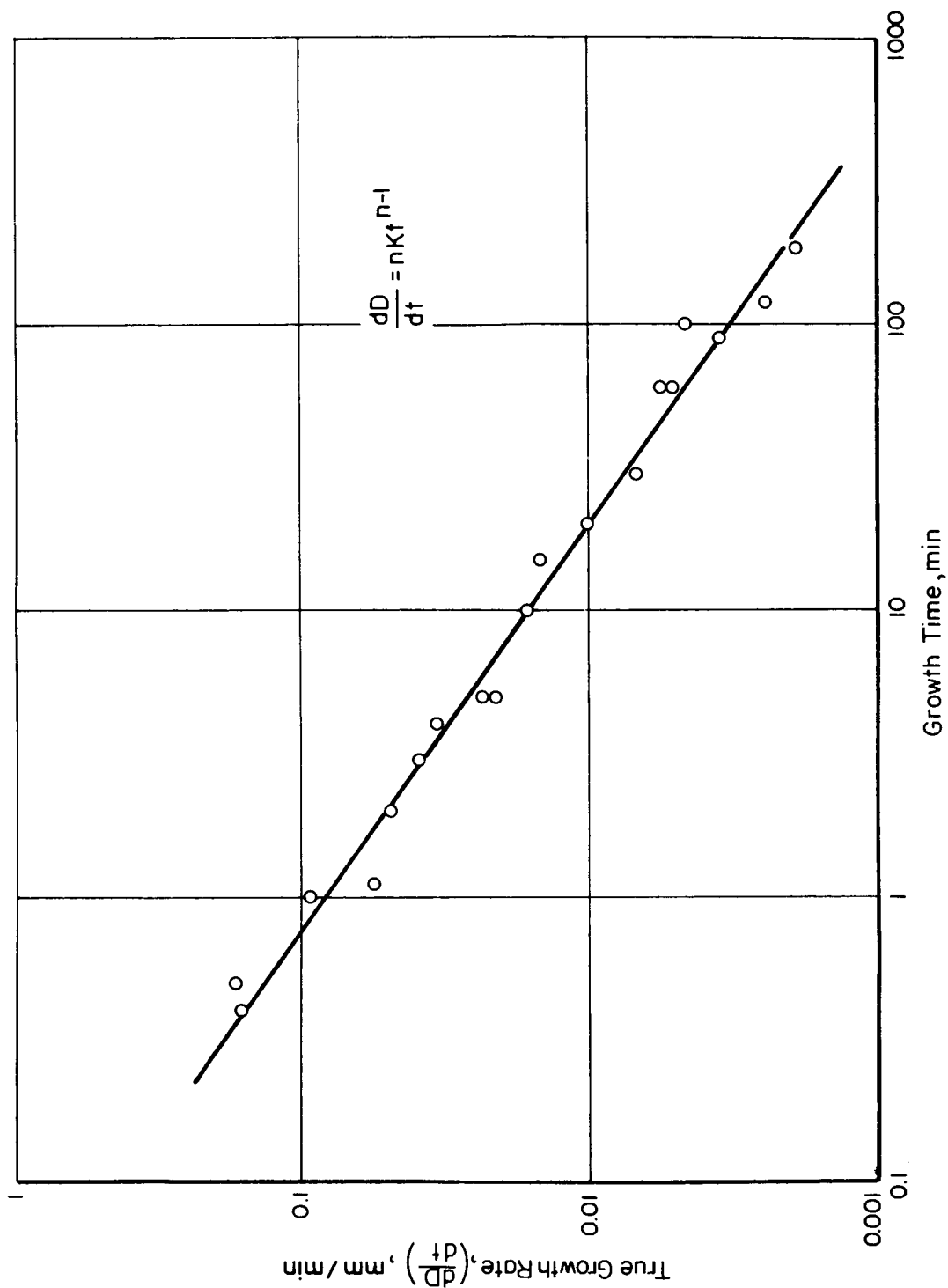


Figure 16.- True growth rate as a function of growth time for Al-10Cu alloys, without applied stress, at 540° C.

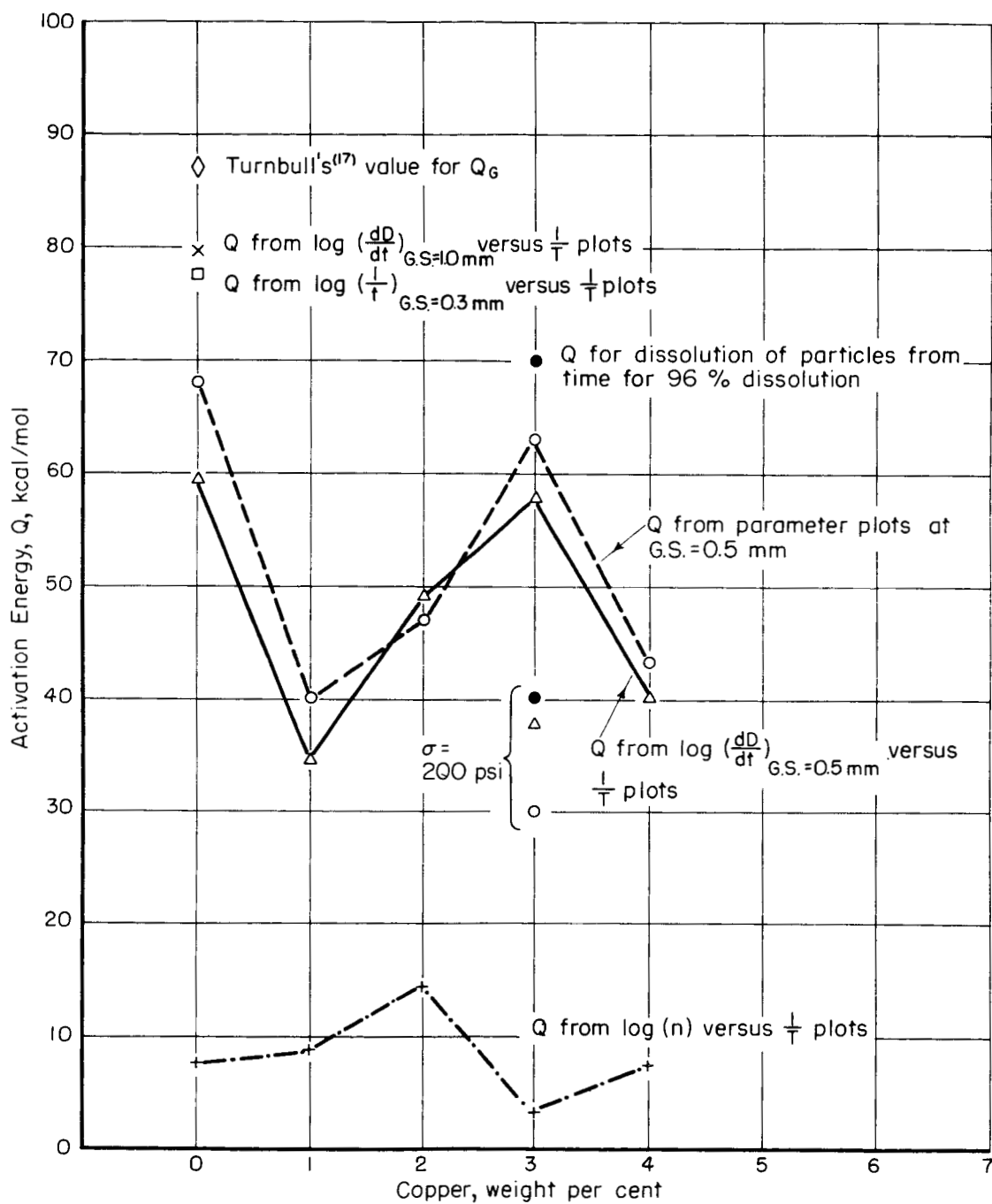


Figure 17.- Relative activation energies of aluminum-copper alloys for grain growth and particle dissolution.

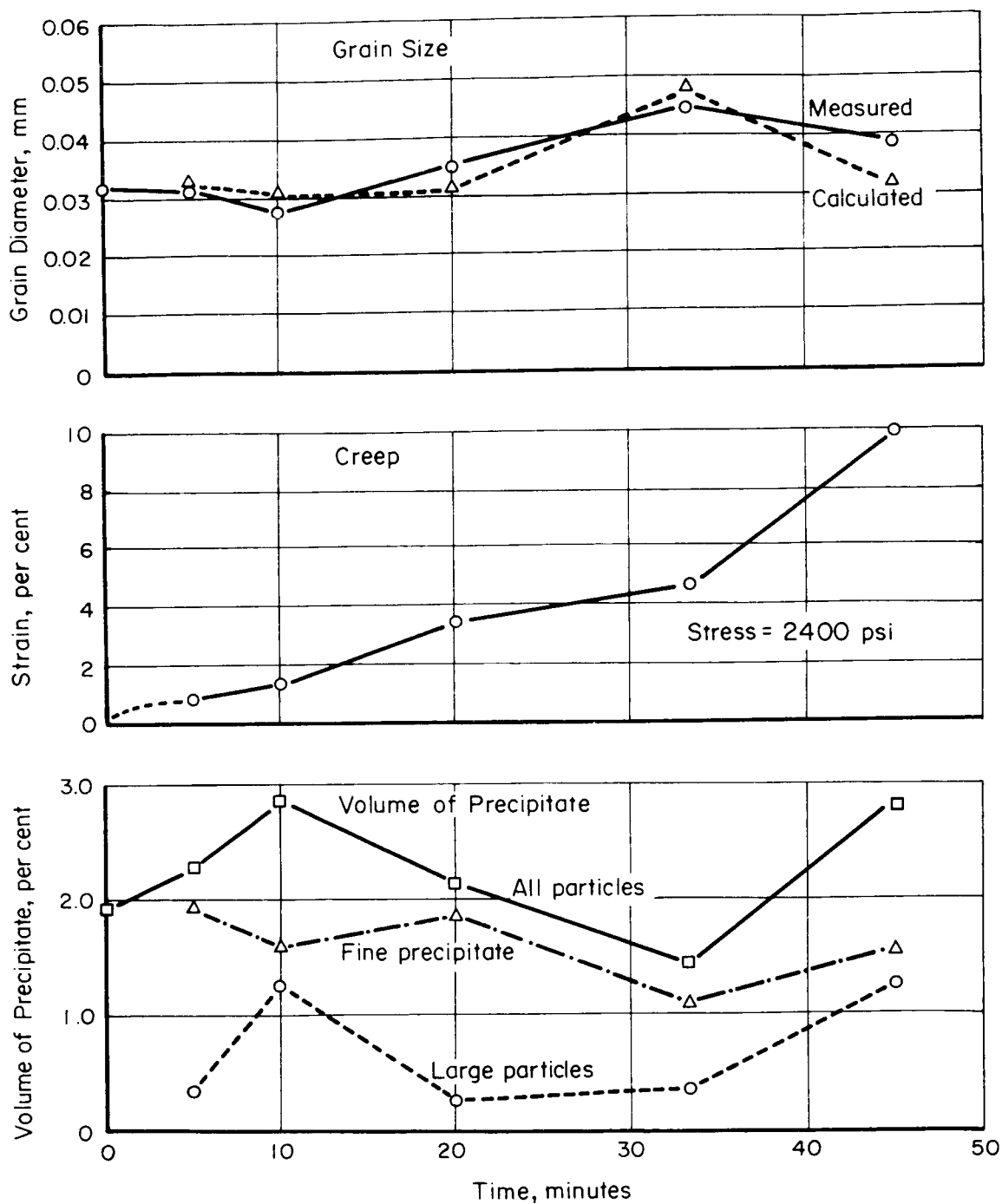


Figure 18.- Precipitation and grain growth during creep of overaged Al-3Cu specimens at 300° C and 2,400 psi.